Berenil [1,3-Bis(4′-amidinophenyl)triazene] Binding to DNA Duplexes and to a RNA Duplex: Evidence for Both Intercalative and Minor Groove Binding Properties†

Daniel S. Pilch, Michael A. Kirolos, Xiaoyan Liu, G. Eric Plum, and Kenneth J. Breslauer*

Department of Chemistry, Rutgers—The State University of New Jersey, New Brunswick, New Jersey 08903

Received March 29, 1995; Revised Manuscript Received June 1, 1995⊗

ABSTRACT: Berenil is an antitrypanosomal agent that binds to nucleic acid duplexes. The generally accepted mode of berenil binding is via complexation into the minor groove of AT-rich domains of DNA double helices. We find that berenil can bind to RNA as well as DNA duplexes, while exhibiting properties characteristic of both intercalation as well as minor groove binding. More specifically, we use spectroscopic, calorimetric, and hydrodynamic techniques to characterize berenil binding to four DNA duplexes and to one RNA duplex. Our results reveal the following features: (i) Berenil binding to the poly[d(A-T)]$_2$, poly(dA)•poly(dT), poly[d(I-C)]$_2$, poly[d(G-C)]$_2$, and poly(rA)•poly(rU) duplexes exhibits intercalative as well as minor groove binding characteristics. (ii) The apparent "site sizes" associated with berenil binding to these five duplexes range from 1 to 13 base pairs per bound berenil and depend, in part, on the host duplex. One of the site sizes common to all five duplexes is consistent with berenil binding to the minor groove. (iii) The apparent berenil binding affinity follows the hierarchy: poly(dA)•poly(dT) > poly-[d(A-T)]$_2$ ≈ poly[d(I-C)]$_2$ ≫ poly(rA)•poly(rU) > poly[d(G-C)]$_2$. (iv) Viscometric data reveal properties characteristic of a significant contribution from an intercalative mode of binding when berenil interacts with the poly[d(A-T)]$_2$, poly[d(I-C)]$_2$, poly[d(G-C)]$_2$, and poly(rA)•poly(rU) duplexes, while revealing an apparent nonintercalative mode when the drug binds to the poly(dA)•poly(dT) duplex. (v) Berenil binding unwinds negative supercoils in the pBR322 plasmid, an observation consistent with an intercalative mode of binding to duplex DNA. (vi) Salt-dependent melting data suggest that both positively charged amidino groups of berenil participate in the complexation of the drug to the poly[d(I-C)]$_2$, poly[d(A-T)]$_2$, poly-(dA)•poly(dT), and poly(rA)•poly(rU) duplexes, while also suggesting that the binding event is site-specific. In the aggregate, our results suggest that, in contrast to the conventional wisdom, berenil can exhibit intercalative as well as minor groove binding properties when it binds to both DNA and RNA duplexes, while also exhibiting a preference for DNA duplexes with unobstructed minor grooves. We comment on the potential correlation between drugs, such as berenil, that exhibit "mixed" binding motifs and those that express anticancer activity via inhibition of topoisomerase I activity.

The interaction of small ligands, such as drugs, with different nucleic acid base sequences and/or structures has been and continues to be the focus of considerable research (Zimmer, 1975; Gale et al., 1981; Marky et al., 1983b; Neidle & Abraham, 1984; Zimmer & Wähnert, 1986; Dervan, 1986; Guschlbauer & Saenger, 1987; Kallenbach, 1988). Much of this interest has centered on the potential use of such nucleic acid binding ligands as gene regulators and/or chemotherapeutic agents. These ligands are able to interact with their nucleic acid hosts by a variety of modes, including intercalation (Neidle & Abraham, 1984) and groove binding (Zimmer & Wähnert, 1986). Appropriately designed biophysical studies can elucidate the mode(s) of ligand binding, the binding affinity, and the nature of the ligand−nucleic acid interactions that give rise to the observed affinities and specificities. Such information can prove of importance in proposing the mechanism(s) of ligand bioactivity and for more rationally designing modified ligands with altered binding properties and biological activities.

Nucleic acid binding ligands generally are classified by the mode by which they interact with their nucleic acid hosts. For example, ethidium is known as a classic intercalator (Neidle & Abraham, 1984), while netropsin is judged to be a classic groove binder (Zimmer, 1975; Zimmer & Wähnert, 1986). These characterizations primarily are based on structural pictures derived from X-ray and/or NMR[1] studies on oligonucleotide−drug complexes. However, several studies have shown that, despite specific classification as an intercalator or a groove binder, some ligands can express binding properties characteristic of more than one binding mode when they complex with their nucleic acid targets (Wells & Larson, 1970; Barton et al., 1986; Zhou et al., 1989; Snyder et al., 1989; Wilson et al., 1990; Tanious et al., 1992; Kamitori & Takusagawa, 1994). In fact, Liu has suggested a correlation between ligands which exhibit such mixed binding modes and those which express anticancer activity

† This work was supported by National Institutes of Health Grants GM23509, GM34469, and CA47995.

* To whom correspondence should be addressed.

⊗ Abstract published in *Advance ACS Abstracts,* July 15, 1995.

[1] Abbreviations: poly[d(A-T)]•poly[d(A-T)], poly[d(A-T)]$_2$; poly-[d(I-C)]•poly[d(I-C)], poly[d(I-C)]$_2$; poly[d(G-C)]•poly[d(G-C)], poly-[d(G-C)]$_2$; poly(rU)•poly(rA)•poly(rU), poly(rA)•2poly(rU); bp, base pair(s); r_{bp}, [total berenil]/[base pairs]; WC, Watson−Crick; DIS, disproportionation; TSS, triplex to single strand; T_m, melting temperature; NMR, nuclear magnetic resonance; CD, circular dichroism; UV, ultraviolet; TLC, thin layer chromatography; EDTA, disodium salt of ethylenediaminetetraacetic acid; DAPI, 4′,6-diamidino-2-phenylindole.

0006-2960/95/0434-9962$09.00/0

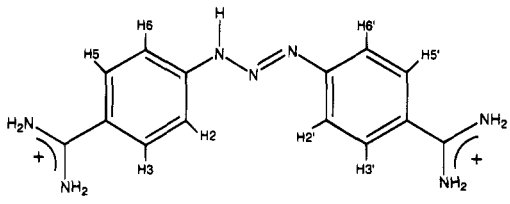

FIGURE 1: Chemical structure of berenil [1,3-bis(4′-amidinophenyl)-triazene] in which the atomic numbering is indicated.

via poisoning of the topoisomerase I−DNA complex (Chen & Liu, 1994). Consequently, the detection and characterization of mixed mode nucleic acid binding ligands, a relatively neglected area, may prove to have some biomedical significance.

In addition to the need to study ligands that bind nucleic acids by multiple modes, there also is a need to characterize ligands that bind to RNA as well as DNA molecules. In fact, an understanding of ligand−RNA recognition patterns is required for the rational design of RNA-binding antiviral drugs (Broder, 1989; Mitsuya et al., 1990) and for the development of RNA-binding ligands that can be used as part of antisense strategies to inhibit selectively the translation of mRNA (Hélène et al., 1985; Stein & Cohen, 1988; Toulmé & Hélène, 1988; Hélène & Toulmé, 1990).

For the reasons noted above, we have begun a program in which we are characterizing the DNA- and RNA-binding properties of various ligands, with particular attention focused on discerning multiple modes of ligand binding. In this work, we employ spectroscopic, calorimetric, and hydrodynamic techniques to assess the nucleic acid binding properties of the antitrypanosomal agent, berenil [1,3-bis(4′-amidinophenyl)triazene] (Figure 1), to four DNA duplexes and to one RNA duplex. Our results reveal that, in contrast to the conventional wisdom, berenil can exhibit intercalative as well as minor groove binding properties when it complexes with DNA and RNA duplexes.

MATERIALS AND METHODS

Nucleic Acid and Drug Molecules. Synthetic DNA and RNA polymers were purchased from either Pharmacia Biotech, Inc. (Piscataway, NJ) or Boehringer Mannheim (Indianapolis, IN) and were used without further purification. Polymers were dissolved to concentrations of approximately 6−7 mM nucleotide with 10 mM sodium cacodylate (pH 6.8). Concentrations of all nucleic acid polymers were determined spectrophotometrically using the following extinction coefficients in units of (mol of nucleotide/L)$^{-1}$ cm^{-1}: ϵ_{262} = 6600 for poly[d(A-T)]·poly[d(A-T)] {≡ poly[d(A-T)]$_2$}, ϵ_{251} = 6900 for poly[d(I-C)]·poly[d(I-C)] {≡ poly[d(I-C)]$_2$}, ϵ_{260} = 6000 for poly(dA)·poly(dT), ϵ_{254} = 8400 for poly[d(G-C)]·poly[d(G-C)] {≡ poly[d(G-C)]$_2$}, ϵ_{258} = 9800 for poly(rA), and ϵ_{260} = 9350 for poly(rU). Solutions containing the poly(rA)·poly(rU) duplex were prepared by mixing poly(rA) and poly(rU) in a 1:1 molar ratio, heating to 90 °C, and then cooling slowly to room temperature in order to minimize formation of competing secondary structures. The plasmid pBR322 was obtained from Boehringer Mannheim and was used without further purification at its extracted superhelical density.

Berenil (97% purity) was obtained from Sigma Chemical Co. (St. Louis, MO). A portion of the berenil was purified to evaluate the impact, if any, of drug purity on the studies conducted here. Purification was accomplished by double recrystallization from ethanol−hexane (Baker & Erickson, 1967), resulting in a species which migrated as a single spot by thin layer chromatography (TLC) in a 6:2.5:1 mixture of n-butanol, distilled water, and glacial acetic acid, respectively. Concentrations of berenil solutions were determined spectrophotometrically using an extinction coefficient in units of M^{-1} cm^{-1} of ϵ_{370} = 34 400 for nonpurified berenil and ϵ_{370} = 36 700 for purified berenil. The extinction coefficient of purified berenil was determined by dry weight and reflects the average of three separate determinations. Control thermal denaturation experiments on purified berenil/DNA complexes yielded virtually identical melting profiles to those in which nonpurified berenil was used. On the basis of these results, all subsequent studies used berenil as received from Sigma, without further purification. Netropsin was obtained from Boehringer Mannheim, while ethidium bromide was obtained from Sigma Chemical Co. Both drugs were used without further purification.

UV Spectrophotometry. Absorbance versus temperature profiles were measured at either 260 or 280 nm on a computer-interfaced Perkin-Elmer model Lambda 4C spectrophotometer equipped with a thermoelectrically controlled cell holder. The heating rate in all experiments was 0.5 °C/min. For each optically detected transition, the melting temperature (T_m) was determined as described previously (Marky & Breslauer, 1987a). Isothermal mixing experiments (Job, 1928; Riley et al., 1966; Pilch et al., 1990) for poly(rA) and poly(rU) established the expected 1:1 stoichiometry corresponding to formation of the poly(rA)·poly(rU) duplex (Krakauer & Sturtevant, 1968).

For the thermal denaturation studies, polyribonucleotide experimental solutions contained 10 mM sodium cacodylate (pH 6.8), 0.1 mM EDTA, RNA at concentrations of either 60 (for measurements at 280 nm) or 20 (for measurements at 260 nm) μM base pair, berenil at concentrations ranging from 0 to 27.6 μM, and NaCl at concentrations ranging from 0 to 800 mM. Polydeoxyribonucleotide experimental solutions, with the exception of those containing poly[d(G-C)]$_2$, contained 10 mM sodium cacodylate (pH 6.8), 0.1 mM EDTA, DNA at a concentration of 30 μM base pair, berenil at concentrations ranging from 0 to 13.8 μM, and NaCl at concentrations ranging from 0 to 2.5 M. Thermal denaturation experiments on poly[d(G-C)]$_2$ were carried out at 280 nm on solutions containing either 2, 3, or 10 mM sodium cacodylate (pH 6.8−7.0), 0.1 mM EDTA, DNA at a concentration of 30 μM base pair, and berenil at concentrations ranging from 0 to 13.8 μM. The pH values for all cacodylate buffer solutions were adjusted by addition of either HCl or NaOH. At Na^+ concentrations >110 mM, heating induces the disproportionation of the poly(rA)·poly(rU) duplex into the poly(rA)·2poly(rU) triplex and single-stranded poly(rA). This transition is observable at 280 nm, although not at 260 nm (Krakauer & Sturtevant, 1968). Hence, melting profiles on poly(rA)·poly(rU) solutions containing Na^+ concentrations exceeding 110 mM also were measured at 280 nm. The cell path length for all the UV studies was 1 cm.

CD Spectropolarimetry. All CD experiments were performed on an Aviv model 60DS spectropolarimeter (Aviv Associates, Lakewood, NJ) equipped with a thermoelectrically controlled cell holder. CD spectra were recorded from 280 to 450 nm in 0.5 nm increments with an averaging time of 5 s. Nucleic acid titrations were performed at 25 °C by incrementally adding aliquots (1.5−50 μL) of concentrated

nucleic acid polymer solutions (≈4 mM base pair) into solutions (2 mL) containing 18.5 μM berenil. With the exception of the poly[d(G-C)]$_2$ titration, the buffer conditions for all the DNA titrations were 10 mM sodium cacodylate (pH 6.8), 300 mM NaCl, and 0.1 mM EDTA. Those for the poly[d(G-C)]$_2$ titration were 2 mM sodium cacodylate (pH 7.0) and 0.1 mM EDTA. Buffer conditions for the RNA titrations were 10 mM sodium cacodylate (pH 6.8), 25 mM NaCl, and 0.1 mM EDTA. The final CD spectra were normalized to reflect equimolar berenil concentrations.

Isothermal Titration Calorimetry. These calorimetric measurements were performed at 25 °C on a Microcal Omega titration calorimeter (Microcal, Inc., Amherst, MA). In a typical experiment, 5 μL aliquots of 2 mM berenil were injected from a 100 μL rotating syringe into an isothermal sample chamber containing 1.35 mL of a nucleic acid solution which was 400 μM in base pairs. The syringe was fitted with a stirrer blade at its end to ensure effective mixing of the sample (Wiseman et al., 1989). The duration of each injection was 8 s, and the delay between injections was 5 min. Each injection generated a heat burst curve (μcal/s vs s). The area under each curve was determined by integration (using the Origin version 1.16 software; Microcal, Inc., Amherst, MA) and provided a measure of the heat of berenil binding for that injection. The calorimeter was calibrated both electronically and chemically. Chemical calibration was achieved by measuring the heat of dilution of 0.3 M NaCl (Robinson, 1932; Gulbransen & Robinson, 1934) with a calibration factor of 1.012 being so determined. Experimental injections resulted in heats ranging from 5 to 65 μcal, depending on the host nucleic acid. The binding enthalpies (ΔH_B) reported in this work reflect the total heat obtained by integration of the peaks resulting from the first two injections divided by the total concentration of injected berenil. These two injections resulted in a [base pair]/[total berenil] ratio ($1/r_{bp}$) of 29.1, at which most of the berenil should be bound considering the value of the binding constants. Heats of dilution corrections were negligible since neither injection of 2 mM berenil into buffer nor buffer into 400 μM base pair nucleic acid resulted in a detectable heat. With the exception of poly[d(G-C)]$_2$ solutions, buffer conditions for experiments on DNA solutions were 10 mM sodium cacodylate (pH 6.8), 300 mM NaCl, and 0.1 mM EDTA. For experiments on poly[d(G-C)]$_2$, the solutions contained 2 mM sodium cacodylate (pH 7.0) and 0.1 mM EDTA. Buffer conditions for experiments on poly(rA)·poly(rU) were 10 mM sodium cacodylate (pH 6.8), 25 mM NaCl, and 0.1 mM EDTA.

Viscometry. Viscosity measurements were conducted in a Cannon-Manning size 75 capillary viscometer (Thomas Scientific, Swedesboro, NJ) submerged in a water bath that was maintained at 24.7 (±0.1) °C. Flow times were measured two to five times to an accuracy of ±0.3 s with a stopwatch, and the average time over all replicates was recorded. Viscosity studies on the plasmid pBR322 were conducted at pH 7.5 in buffer containing 2.6 mM Tris-HCl, 2.0 mM sodium cacodylate, and 0.3 mM EDTA. Aliquots (3 μL) of either berenil, ethidium, or netropsin solutions (2.85 mM) were titrated directly into the viscometer containing solutions (1 mL) of 200 μM nucleotide pBR322, and flow times in the range of 120−140 s were measured after each addition.

Viscosity studies on poly[d(A-T)]$_2$, poly[d(I-C)]$_2$, and poly(dA)·poly(dT) were conducted at pH 6.8 in buffer containing 10 mM sodium cacodylate, 300 mM NaCl, and 0.1 mM EDTA. Aliquots (3 μL) of 3.8 mM berenil were titrated into the viscometer containing polynucleotide solutions (1 mL) of 500 μM base pair, and flow times in the range of 140−330 s were measured after each addition. Studies on poly[d(G-C)]$_2$ were conducted at pH 7.0 in buffer containing 2 mM sodium cacodylate and 0.1 mM EDTA, while those on poly(rA)·poly(rU) were conducted at pH 6.8 in buffer containing 10 mM sodium cacodylate, 25 mM NaCl, and 0.1 mM EDTA. In these studies, aliquots (3 μL) of 7.1 mM berenil were titrated into the viscometer containing polynucleotide solutions (1 mL) of 500 μM base pair, and flow times in the range of 160−230 s were measured after each addition.

NMR Spectrometry. All NMR experiments were conducted on a Varian VXR-500 spectrometer, equipped with an Oxford Instruments magnet. Self-association studies were carried out at pD = 7.2 [pH meter reading of 6.8 plus 0.4 as a correction for the presence of D_2O (Glasoe & Long, 1960)] on D_2O solutions (500 μL) containing 10 mM sodium cacodylate, either 25 or 300 mM NaCl, 0.1 mM EDTA, and berenil at concentrations ranging from to 50 μM to 247 mM. At each berenil concentration, NMR spectra were acquired at temperatures of 10, 25, 45, and 65 °C with an acquisition delay of 1 s.

RESULTS AND DISCUSSION

Berenil Does Not Significantly Self-Associate at Drug Concentrations Below 10 mM. An important first step in the biophysical characterization of a nucleic acid-binding ligand is to determine as a function of solution conditions the aggregation state(s), if any, of the ligand prior to binding. To this end, we monitored the ^{1}H NMR signal of berenil in D_2O as a function of total berenil concentration. These spectra, along with our analysis of the associated data, are provided as Supporting Information. Suffice it to say that our concentration-dependent NMR data reveal that berenil overwhelmingly exists as a monomer under the experimental conditions used in the work described below. In other words, berenil self-association does not interfere with our nucleic acid-binding studies.

Berenil Binds to DNA Duplexes and Enhances Their Thermal Stabilities. Panels A−D of Figure 2 show the UV melting curves for the poly[d(A-T)]$_2$ (panel A), poly(dA)·poly(dT) (panel B), poly[d(I-C)]$_2$ (panel C), and poly[d(G-C)]$_2$ (panel D) duplexes in the absence and presence of differing concentrations of berenil. Note that as r_{bp} increases from 0 to 0.46, the thermal stabilities of all four DNA host duplexes increase concomitantly. These berenil-induced changes in thermal stability are consistent with berenil binding to each of the four DNA duplexes, with a preference for the duplex versus single-stranded state (Crothers, 1971; Neidle & Abraham, 1984; Zimmer & Wähnert, 1986; Snyder et al., 1989). To the best of our knowledge, our observation of ligand-induced changes in the thermal stability of the poly[d(I-C)]$_2$ duplex provides the first demonstration of berenil binding to I·C double-helical sequences.

Inspection of Figure 2 reveals that a much lower ionic strength (2 mM Na^+) is required to observe significant berenil-induced changes in the thermal stability of poly[d(G-C)]$_2$ relative to the other three DNA duplexes (310 mM Na^+). Without necessarily implying a common binding motif to the host duplexes at the different salt concentrations, this

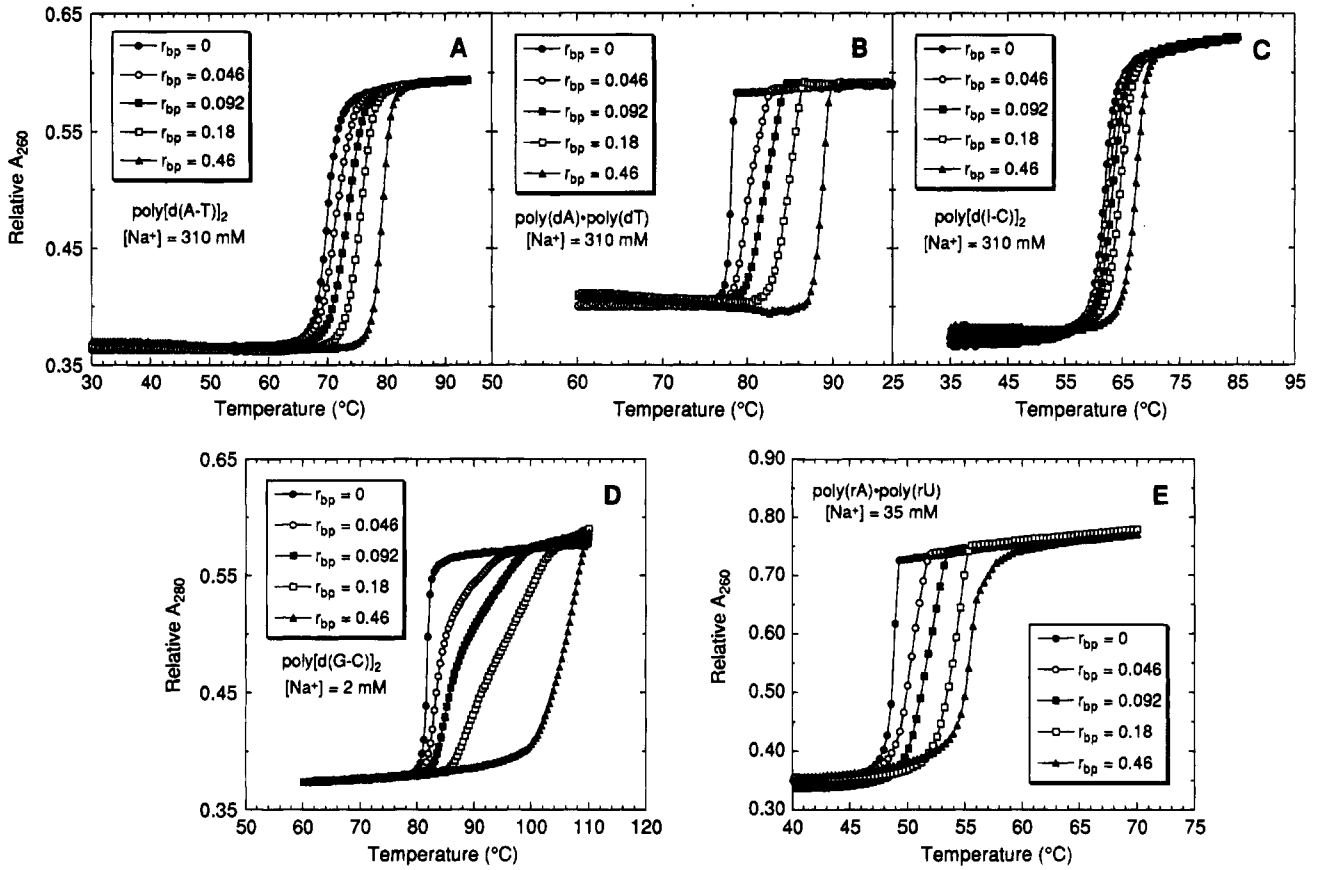

FIGURE 2: UV melting profiles at either 260 or 280 nm of nucleic acid duplexes and their berenil complexes (at the indicated values of r_{bp}) for poly[d(A-T)]$_2$ (A), poly(dA)•poly(dT) (B), poly[d(I-C)]$_2$ (C), poly[d(G-C)]$_2$ (D), and poly(rA)•poly(rU) (E). For studies on poly[d(A-T)]$_2$, poly[d(I-C)]$_2$, and poly(dA)•poly(dT), solution conditions were 10 mM sodium cacodylate (pH 6.8), 300 mM NaCl, and 0.1 mM EDTA. Studies on poly[d(G-C)]$_2$ were conducted at pH 7.0 in a buffer containing 2 mM sodium cacodylate and 0.1 mM EDTA, while those on poly(rA)•poly(rU) were conducted at pH 6.8 in a buffer containing 10 mM sodium cacodylate, 25 mM NaCl, and 0.1 mM EDTA. For clarity of presentation, the melting curves for a given duplex and its berenil complexes were normalized so as to produce identical absorbances at 94 °C [for poly[d(A-T)]$_2$], 98 °C [for poly(dA)•poly(dT)], 85 °C [for poly[d(I-C)]$_2$], 60 °C [for poly[d(G-C)]$_2$], and 85 °C [for poly(rA)•poly(rU)].

observation suggests that nonelectrostatic interactions contribute more when the dicationic ligand binds to the AT- and IC-containing host duplexes than when it binds to the GC-containing host duplex. This conclusion is consistent with the findings of Portugal and Waring (1986, 1987), who demonstrated by DNase I footprinting measurements that berenil binds more strongly to A•T duplex sites relative to G•C duplex sites.

Further inspection of Figure 2 reveals the influence of berenil binding on the thermal stabilities of the poly[d(I-C)]$_2$ and poly[d(A-T)]$_2$ duplexes to be similar. This similarity could be coincidental or it could reflect a component of the binding event which involves interactions of the drug with the accessible ("open") minor grooves of these two host duplexes, which are lined by identical functional groups. We previously have observed such a similarity for netropsin (Marky & Breslauer, 1987b) and for daunomycin (Remeta et al., 1993) binding to these same two duplexes. However, berenil binding appears to be more complex than that of a classic minor groove ligand, such as netropsin, since, as described in a later section, berenil binding also exhibits properties characteristic of intercalation.

Berenil Also Binds to a RNA Duplex and Enhances Its Thermal Stability. Panel E of Figure 2 presents the UV melting curves for the poly(rA)•poly(rU) duplex in the absence and presence of differing concentrations of berenil. Note that, as with the DNA host duplexes, the thermal stability of this RNA duplex increases as r_{bp} increases from 0 to 0.46. Once again, this observation is consistent with berenil preferentially binding to the duplex versus the single-stranded state. Similar ligand-induced increases in the thermal stability of poly(rA)•poly(rU) previously have been observed by Wilson and co-workers (Tanious et al., 1992) for the *intercalating* ligands propidium and quinacrine, while the minor groove-binding ligand distamycin was found to induce no change in thermal stability. This latter result is consistent with (but does not prove) the notion that distamycin does not bind to the RNA duplex. By contrast, Tanious et al. (1992) also found that DAPI (4′,6-diamidino-2-phenylindole), another AT-specific and putative minor groove-binding ligand, does enhance the thermal stability of the poly(rA)•poly(rU) duplex. The authors interpreted this observation as suggesting that DAPI can bind to an RNA duplex by intercalation. Consistent with this view, we describe below measurements which suggest that our observed berenil-induced enhancement in the thermal stability of the poly(rA)•poly(rU) duplex also results, at least in part, from a mode of binding that exhibits viscometric properties characteristic of intercalation. Thus, based on the results of Wilson and co-workers on DAPI (Tanious et al., 1992) and our observations on berenil, it appears that, in contrast to distamycin, these two putative AT-specific, B-form DNA, minor groove-binding ligands also can bind to an all-AU, A-form RNA duplex [poly(rA)•poly(rU)] using a binding

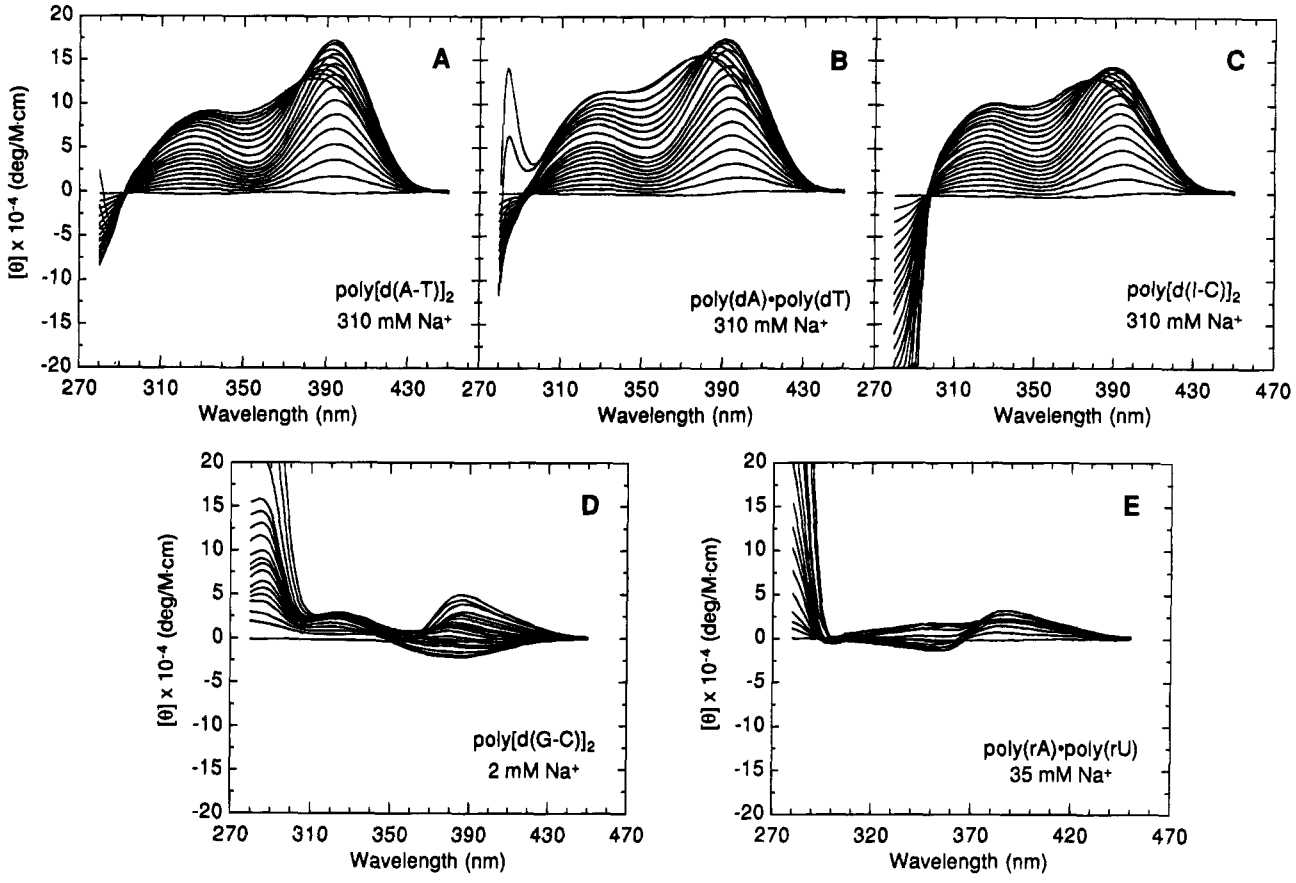

FIGURE 3: CD titrations at 25 °C of berenil (18.5 μM) with poly[d(A-T)]$_2$ (A), poly(dA)•poly(dT) (B), poly[d(I-C)]$_2$ (C), poly[d(G-C)]$_2$ (D), and poly(rA)•poly(rU) (E). From bottom to top, at either 330 nm (for the DNA titrations) or 420 nm (for the RNA titration), the CD spectra correspond to $1/r_{bp}$ ratios of 0 to 23−30. Solution conditions were the same as those described in the legend of Figure 2. Molar ellipticities, [θ], are in units of deg/M•cm, where M refers to moles of total berenil per liter.

mode(s) that exhibits properties characteristic of intercalation.

Inspection of Figure 2 reveals that a lower ionic strength (35 mM Na^+) is required to observe significant berenil-induced changes in the thermal stability of poly(rA)•poly(rU) relative to the three DNA duplexes containing AT or IC base pairs (310 mM Na^+), but not relative to the poly[d(G-C)]$_2$ duplex, which, as noted above, requires an even lower ionic strength (2 mM Na^+). Again, without necessarily implying a common binding motif to the host duplexes at the different salt concentrations, this observation suggests that, relative to the RNA host duplex, nonelectrostatic interactions contribute more when the dicationic ligand binds to the AT- and IC-containing DNA duplexes and less when it binds to the GC-containing DNA duplex. In fact, to gain insight into the RNA state targeted or induced by berenil binding, as well as to define the electrostatic contribution to the binding event, we have determined a complete temperature-, salt-, and berenil-dependent phase diagram for the poly(rA)•poly(rU) duplex. We present these results in the Appendix. This appended material is designed to underscore the importance of such multiparametric characterizations for establishing meaningful comparisons of ligand binding properties over a range of solution conditions.

The results presented above describe our use of UV melting curves to define the influence of berenil binding on the temperature-dependent transitions of DNA and RNA duplexes. In the sections that follow, we describe how circular dichroism (CD) measurements can be used to characterize further the nucleic acid-binding properties of berenil.

CD-Detected Berenil Binding to Duplex DNA Reveals Two Apparent Binding Site Sizes. In addition to the UV thermal denaturation studies described above, CD spectropolarimetry provides a second means for detecting and characterizing ligand binding. Panels A−D of Figure 3 show the CD spectra from 280 to 450 nm obtained by incremental titration of poly[d(A-T)]$_2$ (panel A), poly(dA)•poly(dT) (panel B), poly[d(I-C)]$_2$ (panel C), or poly[d(G-C)]$_2$ (panel D) into a solution of berenil. Neither free berenil nor any of the drug-free duplexes (spectra not shown) exhibit CD signals between 300 and 450 nm. However, upon addition of any one of the duplexes into a berenil solution, substantial CD signals arise in this wavelength range. These induced CD signals exhibit maxima at 330, 380, 385, and/or 390 nm, in a manner that depends on both the host duplex and the $1/r_{bp}$ ratio. These induced CD signals are indicative of interactions between berenil and each of the target duplexes and can be used to detect and to monitor the *CD-active* mode of berenil binding. When a poly[d(G-C)]$_2$ titration identical to that depicted in panel D is conducted in 310 mM Na^+ (data not shown), no induced CD signals are observed. Although the absence of an induced CD signal does not demonstrate a lack of binding, it does mean that at 310 mM Na^+ berenil does not bind to the poly[d(G-C)]$_2$ duplex in a CD-active manner. Thus, when poly[d(G-C)]$_2$ is the host duplex, the CD-active mode of berenil binding can be salted out at 310 mM Na^+, in contrast to when the other three DNA duplexes serve as the hosts.

Further inspection of the CD titration spectra shown in panels A−D of Figure 3 reveals the absence of a single

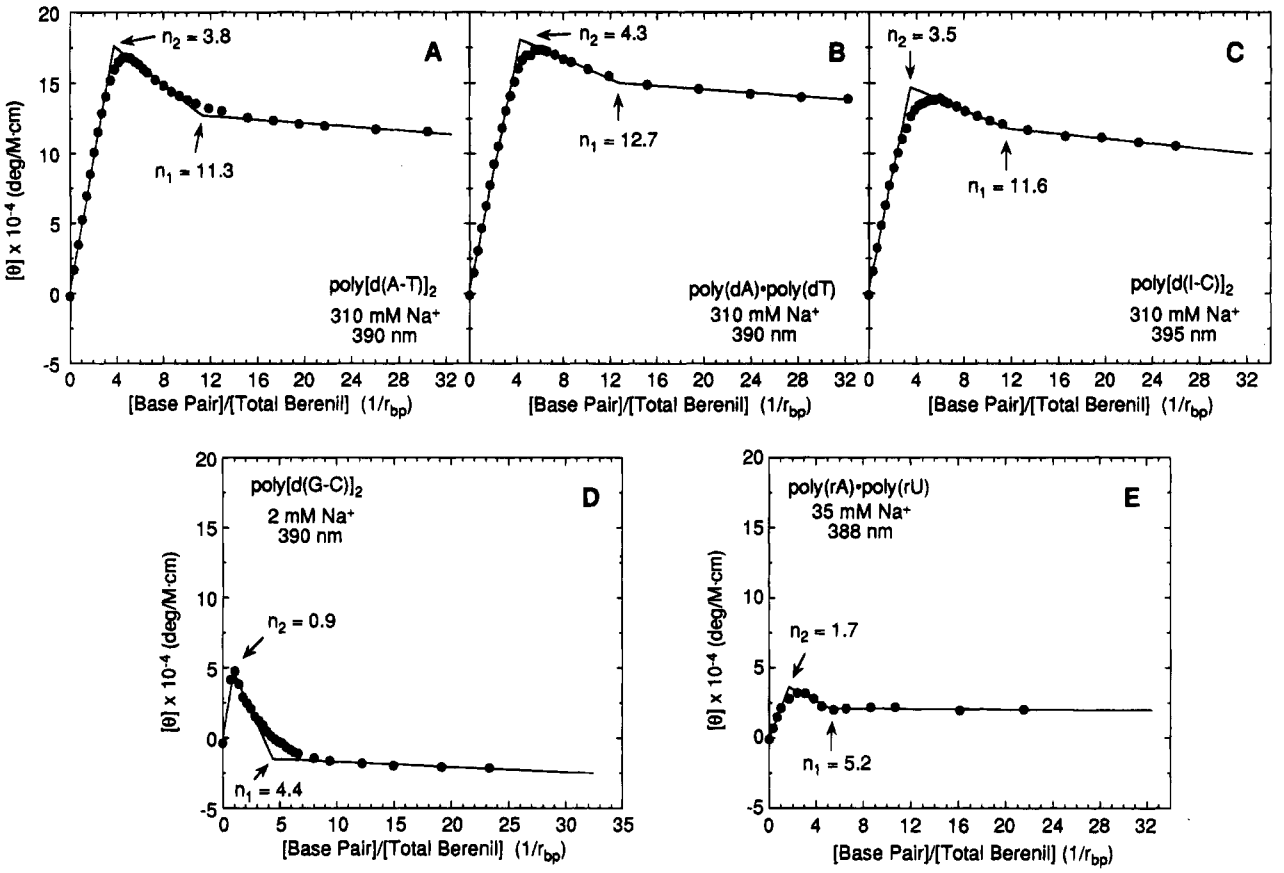

FIGURE 4: Normalized molar (moles of total berenil/liter) ellipticities at the indicated wavelengths versus $1/r_{bp}$ for the titration at 25 °C of berenil with poly[d(A-T)]$_2$ (A), poly(dA)•poly(dT) (B), poly[d(I-C)]$_2$ (C), poly[d(G-C)]$_2$ (D), and poly(rA)•poly(rU) (E). The solid lines reflect linear least-squares fits of the experimental data (filled circles). The apparent binding site sizes (n) in units of base pair(s) per berenil bound which correspond to the inflection points in the fitted lines are indicated. Solution conditions were the same as those described in the legend of Figure 2.

discrete isoelliptic point for any one of the four DNA host duplexes. In fact, for the poly[d(A-T)]$_2$ and poly[d(I-C)]$_2$ duplexes, two isoelliptic points are observed at 293 and 376 nm, while for the poly(dA)•poly(dT) duplex they occur at 295 and 380 nm. The isoelliptic points which occur at either 293 or 295 nm are shared by the spectra which correspond to free berenil and by those which correspond to the drug-bound complexes with $1/r_{bp}$ values ≤ 6. By contrast, the isoelliptic points which occur at either 376 or 380 nm are shared by the drug-bound spectra which correspond to $1/r_{bp}$ values >6. *The absence of a single distinct isoelliptic point for all four duplexes is consistent with more than one optically detectable event when poly[d(A-T)]$_2$, poly[d(I-C)]$_2$, poly(dA)•poly(dT), or poly[d(G-C)]$_2$ serves as the host duplex.* This observation may reflect more than one mode of berenil binding. However, alternatively, it may reflect a single mode of binding with dual characteristics of both intercalation and groove binding which differentially express themselves in a way that depends on the host duplex and/or the binding density ($1/r_{bp}$). Yet another explanation would invoke a binding-induced conformational change in the host duplex. All of these possibilities could, in principle, give rise to the observed lack of a single discrete isoelliptic point.

Single-wavelength titration curves extracted from the CD titration spectra shown in Figure 3 are presented in Figure 4. In these curves, the points represent the experimental molar ellipticities of the drug, while the solid lines reflect linear least-squares fits of the experimental points. Note that two inflection points are observed for berenil binding to all four DNA host duplexes (panels A–D). The presence of two inflection points is consistent with several possible binding models. In one model, the drug binds by a "singular" motif with an apparent site size defined by the first inflection point, while the second inflection point reflects a binding-induced conformational change in the host duplex. In this model, the "singular" berenil binding motif need not be exclusively intercalative or groove binding but can manifest properties characteristic of both modes (e.g., partial intercalation of one ring of the drug, with the other ring residing in the minor groove). A second berenil binding model that could result in two inflection points involves the drug binding by two separate motifs, each with different binding site sizes (e.g., intercalation and groove binding). For the moment, we will not attempt to differentiate between these two possible interpretations of the data. Instead, we simply note that the $1/r_{bp}$ values corresponding to the two inflection points provide estimates for the apparent number of base pairs influenced by each event. These values must be considered lower estimates because $1/r_{bp}$ reflects the ratio of [base pairs] to [total berenil] rather than to [bound berenil]. For the host duplexes used in this study, these $1/r_{bp}$ values are summarized in Table 1. Note that when the poly[d(A-T)]$_2$ (panel A), poly(dA)•poly(dT) (panel B), or poly[d(I-C)]$_2$ (panel C) duplex serves as the host structure, one event influences an apparent site size between 11.3 and 12.7 base pairs per berenil bound, while the other is associated with an apparent site size ranging from 3.5 to 4.3 base pairs per berenil bound. We believe that the smaller size reflects a specific mode of berenil binding to a specific DNA site since it is in agreement with DNase footprinting (Portugal &

Table 1: Apprent Binding Site Sizes Associated with Berenil Interacting with Various Double-Helical Nucleic Acids at 25 °C[a]

host duplex	[Na^+] (mM)	apparent binding site size[b] (base pairs/berenil bound) n_1	n_2
poly[d(A-T)]$_2$	310	11.3 ± 1.1	3.8 ± 0.4
poly[d(I-C)]$_2$	310	11.6 ± 1.2	3.5 ± 0.4
poly[d(G-C)]$_2$	2	4.4 ± 0.7	0.9 ± 0.2
poly(dA)·poly(dT)	310	12.7 ± 1.3	4.3 ± 0.4
poly(rA)·poly(rU)	35	5.2 ± 0.6	1.7 ± 0.2

[a] With the exception of poly[d(G-C)]$_2$, solution conditions for all the DNA measurements were 10 mM sodium cacodylate (pH 6.8), 300 nM NaCl, and 0.1 mM EDTA. The poly[d(G-C)]$_2$ measurements were carried out in 2 mM sodium cacodylate (pH 7.0) and 0.1 mM EDTA. Solution conditions for all the RNA measurements were 10 mM sodium cacodylate (pH 6.9), 25 mM NaCl, and 0.1 mM EDTA. [b] Apparent binding site sizes were determined from the single wavelength, induced CD titration curves ([θ] vs $1/r_{bp}$) shown in Figure 4. These apparent binding site sizes should be considered lower limits since $1/r_{bp}$ reflects the ratio of [base pairs] to [total berenil] rather than to [bound berenil]. Errors reflect the 95% confidence limits obtained from linear regression analyses.

Waring, 1986, 1987), crystallographic (Brown et al., 1990, 1992), and NMR (Yoshida et al., 1990; Shafer et al., 1990; Lane et al., 1991; Jenkins et al., 1993) studies of berenil complexation with duplex DNA. Based on this agreement, it is tempting to ascribe this site size to minor groove binding. However, as noted above, this mode need not be exclusively minor groove binding but also could exhibit properties characteristic of intercalation, as we observe below in our viscometric studies. The binding event associated with the larger apparent site sizes may reflect an allosteric conformational change in the host duplex induced by berenil binding, rather than a specific mode of berenil binding. This type of allosteric behavior previously has been observed in CD studies of DAPI binding to the poly[d(A-T)]$_2$ duplex (Eriksson et al., 1993) as well as in other studies which probe the interactions of ligands such as ethidium, propidium, and daunomycin with the poly(dA)·poly(dT) duplex (Wilson et al., 1985; Breslauer et al., 1987; Herrera & Chaires, 1989; Scaria & Shafer, 1991).

In contrast to the behavior noted above, the two inflection points in the poly[d(G-C)]$_2$ titration curve (panel D of Figure 4) correspond to apparent "binding" site sizes of 4.4 and 0.9 base pairs per berenil bound. The first of these apparent binding site sizes (4.4) is quantitatively similar to the smaller of the two classes observed with the other three DNA duplexes (3.5−4.3). Again, it is tempting to assign this site size to minor groove binding. However, our viscometric measurements (see below) reveal that berenil binding to the poly[d(G-C)]$_2$ duplex with this site size also exhibits viscometric properties characteristic of intercalation. The second apparent site size for poly[d(G-C)]$_2$ is quite different compared with the other three DNA host duplexes (0.9 as opposed to either 3.5−4.3 or 11.3−12.7 base pairs per berenil bound). This smaller binding site size (0.9) may correspond to a secondary mode of berenil binding in which electrostatically driven stacking of the drug on the helix exterior occurs under conditions of high drug loading (low $1/r_{bp}$ ratios). Such a binding mode would be enhanced under conditions of low ionic strength, as used in the poly[d(G-C)]$_2$ titration (2 mM Na^+), and would result in very few base pairs being covered per bound drug molecule. This secondary binding motif, in fact, is common among DNA intercalating ligands (Neidle & Abraham, 1984).

Comparison with Previous Berenil Binding Studies to DNA Duplexes. With one relatively recent exception (Schmitz & Hübner, 1993), all previous studies on the interactions of berenil with duplex DNA report the detection of only one mode of berenil binding, with a binding site size of approximately 4−5 base pairs per berenil bound. These studies include characterizations by NMR (Shafer et al., 1990; Yoshida et al., 1990; Lane et al., 1991; Jenkins et al., 1993), crystallography (Pearl et al., 1987; Brown et al., 1990, 1992), fluorometry (Braithwaite & Baguley, 1980), spectrophotometry (Newton, 1967; Barceló & Portugal, 1993), viscometry (Newton, 1967), sedimentation velocity (Waring, 1970), and DNase footprinting (Portugal & Waring, 1986, 1987). As noted above, one of the two classes of apparent binding site sizes observed in this work (3.5−4.4 base pairs) is very close to the value found in these previous studies.

Barceló and Portugal (1993) report that berenil exhibits only a single binding event when complexed with either the poly[d(A-T)]$_2$ or the poly(dA)·poly(dT) duplex. These authors used UV absorption spectroscopy to generate single-wavelength titration curves which they found to contain only one observable inflection point, from which their binding stoichiometries were extracted. We observe similar results when employing this spectroscopic technique to generate such titration curves (data not shown). However, we also find that only the absorption spectra which correspond to $1/r_{bp} \leq 6$ pass through the sole observable isosbestic point at 382 nm. In addition, as noted above, we observe two distinct inflection points in the CD titration curves (Figure 4, panels A and B), although this latter behavior depends on the wavelength monitored. These differential observations highlight the importance of using multiple spectroscopic techniques over a broad range of wavelengths to characterize the binding stoichiometry(ies) of nucleic acid−ligand complexes.

The results of a recent UV absorption study by Schmitz and Hübner (1993) on the binding of berenil to the poly[d(A-T)]$_2$ and poly(dA)·poly(dT) duplexes contrast with those of Barceló and Portugal (1993) in that they suggest that berenil exhibits two modes of binding when it complexes with these two host duplexes. In both studies, UV absorption spectroscopy was used to monitor berenil binding. However, in the Schmitz and Hübner (1993) study, Scatchard plots derived from the UV data could not be satisfactorily fit by conventional equations designed to describe a single mode of binding to a homogeneous polymer lattice, such as that proposed by McGhee and von Hippel (1974). Better fits were obtained by Schmitz and Hübner (1993) when they used equations modified to reflect two distinct binding events. Their qualitative conclusion regarding two modes of berenil binding when the poly[d(A-T)]$_2$ and poly(dA)·poly(dT) duplexes serve as the hosts is consistent with our CD-derived results, although, as discussed above, one need not require two *distinct* binding events to rationalize the presence of two inflection points or the absence of an isoelliptic point. One of the two classes of apparent binding site sizes defined by Schmitz and Hübner (1993) at 153 mM Na^+ [4 base pairs for poly[d(A-T)]$_2$ and 3 base pairs for poly(dA)·poly(dT)] is consistent with that determined in this study at 310 mM Na^+ [3.8 base pairs for poly[d(A-T)]$_2$ and 4.3 base pairs for poly(dA)·poly(dT)]. However, the second class of binding site size they report for each duplex structure [35 base pairs for poly[d(A-T)]$_2$ and 8 base pairs for poly(dA)·poly(dT)] differs markedly from that reported here [11.3 base pairs

for poly[d(A-T)]$_2$ and 12.7 base pairs for poly(dA)·poly(dT)]. We suggest three factors that may, in part, contribute to these discrepancies. First, our UV studies reveal that, for drug binding to the poly[d(A-T)]$_2$ or poly(dA)·poly(dT) duplex, the berenil extinction coefficients at 402 nm are measurably different for the two site sizes. Schmitz and Hübner (1993) assumed these extinction coefficients to be identical. Second, Schmitz and Hübner (1993) employ a mutual exclusion model (Schwarz & Stankowski, 1979) to describe the binding of berenil to these polymers. This model implies that both binding events are mutually exclusive and are characterized by similar binding affinities, an assumption not likely to hold should berenil binding induce an allosteric conformational change in the poly[d(A-T)]$_2$ and poly(dA)·poly(dT) duplexes. Third, the fits carried out by Schmitz and Hübner (1993) used six free-floating parameters (two binding constants, two binding site sizes, and two cooperativity parameters) and might not converge to the global minimum. Such local minima problems, which affect any fitting program, may be alleviated, in part, by estimating experimentally as many of the parameters as possible. In our study, we used CD titration curves to define lower estimates for the apparent binding site sizes, thereby allowing us to calculate apparent binding constants without curve fitting.

CD-Detected Berenil Binding to a RNA Duplex Also Reveals Two Binding Site Sizes. Panel E of Figure 3 shows the CD spectra from 280 to 450 nm obtained by titration of the poly(rA)·poly(rU) duplex into a solution of berenil at 35 mM Na^+. Note that, as observed for the DNA duplexes, addition of the RNA duplex into a berenil solution induces a CD signal between 300 and 450 nm, consistent with berenil also binding to this host structure. To the best of our knowledge, this is the first report of berenil binding to a RNA duplex. Further note that the family of CD spectra obtained from this titration does not exhibit a single isoelliptic point. The absence of an isoelliptic point is consistent with *more than one optically detected event when poly(rA)·poly(rU) serves as the host duplex.* The same potential explanations can be offered for this observation as were presented above for berenil binding to the DNA host duplexes.

Panel E of Figure 4 shows the single-wavelength titration curve derived from the family of CD spectra shown in Panel E of Figure 3. The two inflection points observed in this titration curve at 5.2 and 1.7 base pairs per berenil bound are consistent with any one of the several binding models described above for the DNA host duplexes. As with the DNA duplexes, we propose that the apparent binding site size of 5.2 is associated with the primary mode of berenil binding. However, as noted above, one should not blindly assume that this mode exclusively is minor groove binding since our viscometric measurements (see below) reveal that berenil binding to poly(rA)·poly(rU) exhibits properties characteristic of intercalation. The smaller binding site size (1.7) may reflect a secondary berenil binding mode which involves electrostatically facilitated stacking along the helix exterior, as was noted for the poly[d(G-C)]$_2$ duplex. This latter possibility is not unreasonable given the relatively low ionic strength at which the poly(rA)·poly(rU) CD titration was conducted (35 mM Na^+).

Relative Berenil Binding Affinities for Duplex Structures Derived from UV Melting Data. As noted above, our CD titrations (see Figures 3 and 4) are consistent with more than one binding event when berenil binds to the nucleic acid duplexes studied here. However, such CD data do not allow one to resolve unambiguously the molar ellipticities corresponding to the different bound forms of berenil. The absence of such information preclude one from constructing Scatchard plots that can yield meaningful binding constants. Alternatively, we describe below how UV-derived T_m data can be used to obtain a quantitative estimate of the apparent berenil binding affinities.

Assuming that berenil binding to the single strands is negligible, an assumption consistent with the results of our induced CD melting studies (not shown), we can calculate the apparent berenil duplex association constants at the T_m ($K_{app}^{T_m}$) using the equation (Crothers, 1971):

$$\frac{1}{T_m^\circ} - \frac{1}{T_m} = \frac{R}{n_D(\Delta H_{WC})} \ln[1 + (K_{app}^{T_m})a_{WC}^B] \qquad (1)$$

where T_m° and T_m are the melting temperatures (in Kelvin) of the UV melting curves in the absence and presence of berenil, respectively, ΔH_{WC} is the enthalpy change for the melting of a WC base pair in the absence of bound ligand, n_D is $1/r_{bp}$ at saturation of the duplex, and a_{WC}^B is the free berenil activity for a WC transition, which can be estimated by one half the total berenil concentration. For meaningful comparisons, the calculated apparent binding constants at T_m should be extrapolated to a common reference temperature using the standard relationship

$$\frac{\partial[\ln(K_{app})]}{\partial\left[\frac{1}{T}\right]} = -\frac{\Delta H_B}{R} \qquad (2)$$

where ΔH_B is the enthalpy of berenil binding.

Note that the binding model described by eq 1 does not distinguish between ligands with differing binding site sizes. Furthermore, for ligands with binding site sizes >1, this model only allows for ligands to bind at regularly spaced intervals of n base pairs. This Scatchard approximation does not account for overlapping binding sites. Hence, ligand binding must be sufficiently tight so as to ensure complete saturation of the host duplex at $1/r_{bp}$ ratios equivalent to n_D. Given these limitations, apparent binding constants determined through use of eq 1 may underestimate those determined by other methods which are not restricted by such limitations. However, in several previous studies (Remeta et al., 1993; Snyder et al., 1989; Snyder, 1989), we found good agreement between drug binding constants determined by this "ΔT_m method" and those measured by more direct techniques, thereby providing us with confidence in this approach.

Table 2 summarizes the apparent association constants at 25 °C ($K_{app}^{25°C}$), that we have calculated using eqs 1 and 2, for berenil binding to the poly[d(A-T)]$_2$, poly[d(I-C)]$_2$, poly(dA)·poly(dT), and poly(rA)·poly(rU) host duplexes over a range of Na^+ concentrations. For each duplex, the tabulated T_m values were measured at $1/r_{bp}$ ratios which correspond to the primary mode of berenil binding (in the range of 3.5−5.2 base pairs per bound berenil; see Table 1). The high thermal stability of the poly[d(G-C)]$_2$ duplex at Na^+ concentrations above 2−3 mM prevented us from determining $K_{app}^{T_m}$ values for berenil binding to this duplex. Berenil binding enthalpies required for extrapolation of the binding constants to a common reference temperature using eq 2 were determined for all the duplexes studied here using isothermal titration calorimetry. These data are listed in Table 3. It is

Table 2: Salt Dependence of the Apparent Association Constants at 25 °C ($K_{app}^{25°C}$) for Berenil Binding to Various Double-Helical Nucleic Acids

[Na^+] (M)	T_m° [a] (°C)	T_m [a] (°C)	$K_{app}^{25°C}$ [a] (M^{-1})
	poly[d(A-T)]$_2$		
0.010	38.2	78.3	7.3×10^7
0.018	45.1	78.5	3.2×10^7
0.035	51.8	77.8	1.3×10^7
0.060	56.8	77.1	6.6×10^6
0.110	62.0	78.3	4.0×10^6
	poly[d(I-C)]$_2$		
0.010	32.2	66.0	2.1×10^8
0.018	39.2	66.3	6.5×10^7
0.035	45.7	66.2	2.1×10^7
0.060	50.4	65.6	8.5×10^6
0.110	55.4	65.7	3.5×10^6
	poly(dA)•poly(dT)		
0.010	46.6	87.0	8.8×10^8
0.018	52.2	86.4	2.5×10^8
0.035	58.6	85.9	7.0×10^7
0.060	64.3	85.3	2.1×10^7
0.110	69.9	85.2	7.1×10^6
	poly(rA)•poly(rU)[b]		
0.010	35.0	49.0	1.2×10^7
0.018	41.8	51.8	4.8×10^6
0.035	48.8	53.9	1.4×10^6
0.060	53.8	55.9	4.4×10^5
0.110	58.9	59.3	7.6×10^4

[a] T_m° = melting temperature of the nucleic acid duplex in the absence of berenil. T_m = melting temperature of the berenil/duplex complex at the following $1/r_{bp}$ values: 3.8 for poly[d(A-T)]$_2$, 3.5 for poly[d(I-C)]$_2$, 4.3 for poly(dA)•poly(dT), and 5.2 for poly(rA)•poly(rU). $K_{app}^{25°C}$ values were calculated using eqs 1 and 2 as described in the text. For application of eq 1, the following calorimetrically determined ΔH_{WC} values (in units of kcal/mol base pair) for the melting of a base pair were used: ΔH_{WC} = 7.6 (Chou, 1990) for poly[d(A-T)]$_2$, ΔH_{WC} = 11.4 (Chou, 1990) for poly[d(I-C)]$_2$, ΔH_{WC} = 9.7 (Park, 1992) for poly(dA)•poly(dT), and ΔH_{WC} = 7.9 (Chou, 1990) for poly(rA)•poly(rU). For application of eq 2, the appropriate berenil binding enthalpies (ΔH_B) listed in Table 3 were used. [b] The presence of a small amount of secondary berenil binding ($1/r_{bp}$ = 1.7) may accompany primary binding ($1/r_{bp}$ = 5.2) to poly(rA)•poly(rU), thereby resulting in a slight overestimation of ΔT_m, which, in turn, would lead to a corresponding overestimation of $K_{app}^{25°C}$.

Table 3: Binding Enthalpies for Berenil Complexation with Various Double-Helical Nucleic Acids[a]

host duplex	[Na^+] (mM)	ΔH_B[b] (kcal/mol)
poly[d(A-T)]$_2$	310	-4.8 ± 0.5
poly[d(I-C)]$_2$	310	-6.4 ± 0.7
poly[d(G-C)]$_2$	2	-2.2 ± 0.4
poly(dA)•poly(dT)	310	-2.3 ± 0.4
poly(rA)•poly(rU)	35	-3.0 ± 0.6

[a] Experimental conditions were as stated in the footnote to Table 1. [b] ΔH_B is the enthalpy of berenil binding to the host nucleic acid, as measured directly by titration calorimetry. In all cases, binding enthalpies were determined at $1/r_{bp}$ values of 29.1 and are expressed in units of kcal per mole of injected berenil. Errors reflect single standard deviations from multiple electronic calibration experiments, in which the heat pulses were similar in magnitude to the experimentally measured heats.

interesting to compare these enthalpies for berenil binding with those we previously have reported (Breslauer et al., 1987; Chou et al., 1987; Jin, 1989; Marky et al., 1987b; Remeta et al., 1991, 1993) for the binding of ethidium, a classic intercalator, and netropsin, a classic minor groove binder, to the corresponding four DNA host duplexes. (The relevant data for the one RNA duplex listed in Table 3 has yet to be reported.) This comparison reveals berenil binding to the three alternating DNA copolymers (poly[d(A-T)]$_2$, poly[d(I-C)]$_2$, and poly[d(G-C)]$_2$) to be significantly less exothermic (less favorable) than the corresponding binding of either ethidium or netropsin. In other words, exclusively on the basis of the binding enthalpy data, berenil does not "behave" like a pure intercalator or a pure groove binder. By contrast, when the homopolymeric DNA duplex poly(dA)•poly(dT) serves as the host, we find that the three drugs exhibit similar binding enthalpies. We recognize that there is no necessary correlation between the binding enthalpy of a ligand and its binding mode(s). However, as an aside, it is interesting to note the enthalpic distinctions we observe for berenil, ethidium bromide, and netropsin binding to common DNA duplexes.

Inspection of the data in Table 2 reveals that berenil exhibits similar apparent binding affinities for both the poly[d(A-T)]$_2$ and poly[d(I-C)]$_2$ duplexes. We previously have observed this behavior for other ligands, such as the minor groove binder netropsin (Marky & Breslauer, 1987b) and the intercalator daunomycin (Remeta et al., 1993). In both of these cases, we argued that the similarity was consistent with both duplexes possessing similar global structures (Arnott et al., 1974) and accessible ("open") minor grooves lined by identical functional groups (Remeta et al., 1993). Further inspection of the data in Table 2 reveals that, depending on the Na^+ concentration, berenil exhibits an approximately 2−12-fold higher apparent binding affinity for the poly(dA)•poly(dT) duplex than for the poly[d(A-T)]$_2$ duplex. This result differs from that reported by Schmitz and Hübner (1993), who interpreted their data as suggesting that berenil has a similar apparent binding affinity for the poly[d(A-T)]$_2$ and poly(dA)•poly(dT) duplexes. Furthermore, their reported $K_{app}^{25°C}$ values for berenil binding to poly[d(A-T)]$_2$ are approximately one order of magnitude lower than those we report in Table 2. These discrepancies may arise in part from differences in the method of analysis and/or differences in the heating rates used in the UV melting experiments (1 °C/min in their study as opposed to 0.5 °C/min in this study). The latter possibility is consistent with the fact that our ΔT_m values are significantly greater than theirs.

Berenil Binding to DNA versus RNA Duplex Structures. Inspection of the data in Table 2 reveals that, at a common salt concentration, berenil exhibits substantially greater apparent binding affinities for the three DNA duplexes [poly[d(A-T)]$_2$, poly[d(I-C)]$_2$, and poly(dA)•poly(dT)] relative to the one RNA duplex [poly(rA)•poly(rU)] studied here. Specifically, we find the following hierarchy for berenil binding: poly(dA)•poly(dT) > poly[d(A-T)]$_2$ ≈ poly[d(I-C)]$_2$ ≫ poly(rA)•poly(rU). Conformational differences between B-like DNA duplexes and A-like RNA duplexes (including the topologies of the grooves) may contribute to these differences in apparent binding affinities.

As noted earlier, the high thermal stability of the poly[d(G-C)]$_2$ duplex precluded us from calculating its berenil binding affinity. However, CD studies (data not shown) indicate that the induced CD signal of berenil when bound to poly[d(G-C)]$_2$ is substantially more salt-sensitive than the induced CD signal of berenil when bound to poly(rA)•poly(rU). If one assumes that the salt-dependent induced CD data reflect true thermodynamic binding affinities, then poly[d(G-C)]$_2$ exhibits an even lower affinity for berenil than does the poly(rA)•poly(rU) duplex. If this conclusion is valid,

then the minor groove accessibility of the host duplex could be as important as the global duplex conformation in dictating berenil binding affinity. Clearly, the berenil binding properties of additional RNA and DNA duplexes must be investigated to differentiate between these possibilities.

A more direct assessment of the differential berenil binding properties of DNA versus RNA host duplexes which minimizes base composition effects can be achieved by comparing the poly(dA)·poly(dT) and poly(rA)·poly(rU) berenil binding data. At common salt concentrations, this comparison reveals a significant preference (47−93-fold) for the DNA duplex over the RNA duplex. Clearly, the berenil binding properties of the poly(rA)·poly(rT) duplex also should be examined to provide a more direct comparison. We are aware of the fact that homopolymeric duplexes such as poly(dA)·poly(dT) can assume aberrant, noncanonical conformations which could compromise this comparison (Arnott et al., 1983; Arnott & Selsing, 1974). Clearly, the berenil binding properties of additional DNA and RNA duplexes must be studied to assess the generality of the apparent DNA preference observed here. Nevertheless, one should note that the specific magnitude of the DNA preference depends on the Na^+ concentration. In fact, as discussed in the Appendix, salt-dependent measurements provide a means of evaluating the electrostatic contribution to berenil binding (Record et al., 1976, 1978; Manning, 1978). Qualitatively speaking, we find that berenil binds site specifically as a dication to all five duplexes studied, with the quantitative extent of the electrostatic contribution to binding being dependent on the specific host structure (see the Appendix for details).

In the next section, we use viscometric techniques to characterize further the nature of the modes by which berenil binds to the DNA and RNA duplex structures studied here.

Viscometric Measurements Suggest That Berenil, at Least in Part, Intercalates into the Poly[d(A-T)]$_2$, Poly[d(I-C)]$_2$, Poly[d(G-C)]$_2$, and Poly(rA)·poly(rU) Duplexes, While Binding to the Poly(dA)·poly(dT) Duplex by an Apparent Non-intercalative Mode. The primary mode of binding by which a ligand interacts with a polymeric host nucleic acid structure may be investigated by a number of methods, including fluorescence energy transfer, fluorescence quenching, and viscometry. Both free and nucleic acid-bound berenil have extremely low fluorescence quantum yields (data not shown) and are therefore not well suited to fluorescence studies. Thus, we chose viscometry as a means of investigating the mode by which berenil interacts with nucleic acid duplexes.

If one treats DNA or RNA as a rodlike molecule and assumes negligible changes in the axial ratio upon ligand binding (Cohen & Eisenberg, 1969), the relationship between the relative solution viscosity (η/η_o) and the relative contour length (L/L_o) is given by the expression (Müller & Crothers, 1968; Bloomfield et al., 1974):

$$\frac{L}{L_o} = \sqrt[3]{\frac{\eta}{\eta_o}} \qquad (3)$$

where L_o and η_o denote the apparent molecular length and solution viscosity in the absence of ligand. Based on this equation, an increase in relative viscosity generally reflects an increase in apparent molecular length. Ligand insertion between stacked bases within a linear host duplex (intercalation) is associated with a lengthening of the nucleic acid. Thus, a ligand-induced increase in the viscosity of a duplex

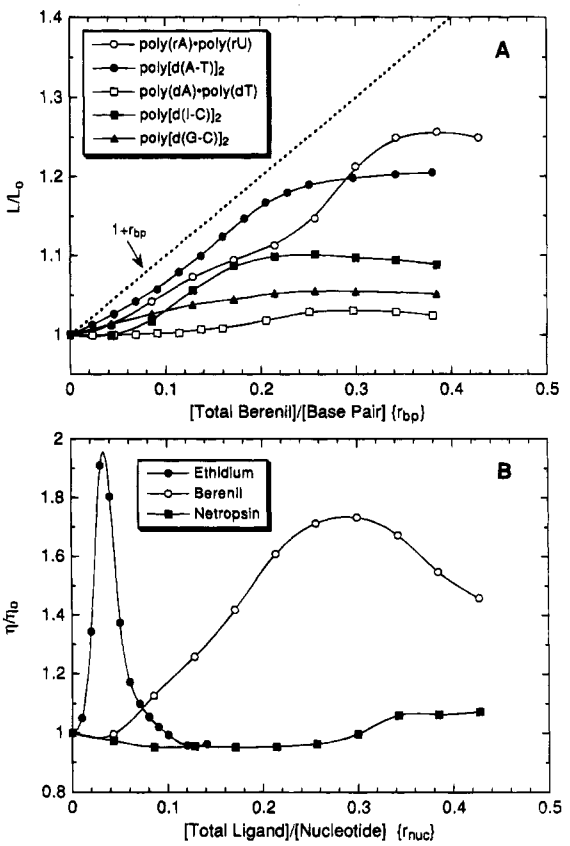

FIGURE 5: (A) Viscometric berenil titrations at 24.7 °C of the poly(rA)·poly(rU) (open circles), poly[d(A-T)]$_2$ (filled circles), poly(dA)·poly(dT) (open squares), poly[d(I-C)]$_2$ (filled squares), and poly[d(G-C)]$_2$ (filled triangles) duplexes. L/L_o is the relative contour length of the host duplex and is defined in the text. The dashed line reflects the theoretical curve ($1+r_{bp}$) predicted by the classic model for intercalation into a rod-like nucleic acid molecule (Lerman, 1961; Cohen & Eisenberg, 1969). Solution conditions were the same as those described in the legend of Figure 2. (B) Viscometric titrations at 24.7 °C of pBR322 with ethidium bromide (filled circles), berenil (open circles), and netropsin (filled squares). η/η_o is the relative solution viscosity and is defined in the text. Solution conditions were 2.6 mM Tris-HCl, 2.0 mM sodium cacodylate, 0.3 mM EDTA, and pH 7.5.

nucleic acid solution is consistent with (but does not prove) an intercalative mode of binding.

Figure 5, panel A, shows the effect of berenil binding on the apparent relative contour lengths of the five host duplexes studied here. Due to the salt-sensitive character of berenil binding to the poly(rA)·poly(rU) and poly[d(G-C)]$_2$ duplexes, the viscosity titrations with these two duplexes had to be performed at lower ionic strengths [2 mM Na^+ for poly[d(G-C)]$_2$ and 35 mM Na^+ for poly(rA)·poly(rU)] than the 310 mM Na^+ used for the viscosity titrations with the other three duplexes. Inspection of Figure 5 reveals that, *upon addition of berenil, the poly[d(A-T)]$_2$, poly[d(I-C)]$_2$, poly[d(G-C)]$_2$, and poly(rA)·poly(rU) duplexes each undergo substantial increases in apparent contour length, suggestive of some degree of berenil intercalation into these four duplexes under the solution conditions employed.* Recall that the conventional wisdom is that berenil is a minor groove-binding ligand that is specific for AT-rich regions of B-form DNA duplexes. We find that berenil can bind to DNA duplexes with accessible minor grooves, to a DNA duplex with a sterically blocked minor groove, and to a RNA duplex, while in all cases exhibiting viscometric properties characteristic of an intercalative contribution to the binding event.

Although the contour lengths of all four duplexes increase in response to berenil binding, inspection of Figure 5, panel A, reveals that the extent of this increase differs markedly from one duplex to the other, with the poly[d(G-C)]$_2$ duplex undergoing the smallest binding-induced increase in contour length. Furthermore, the observed increases in length fall short of the theoretical value of 1 + r_{bp} predicted by the classic model for intercalation into a rod-like nucleic acid molecule (Lerman, 1961; Cohen & Eisenberg, 1969). Several factors may account for these quantitative differences. First, competing nonintercalative binding modes (Jones et al., 1980), such as groove binding and electrostatically facilitated stacking at the helix exterior, may reduce the amount of intercalative binding and therefore the extent of helix lengthening. This type of mixed mode binding competition might be particularly evident at low ionic strength, such as that used in the poly[d(G-C)]$_2$ experiment. Second, structural differences between the intercalated complexes (Waring, 1971) may result in differing degrees of helix lengthening. If one rather than both of the amidinophenyl moieties of berenil intercalates, the second amidinophenyl moiety would be free to interact with the helix elsewhere, perhaps in the minor groove. This type of partially intercalated complex, where one amidinophenyl group is intercalated within the helical stack and the other interacts in the minor groove, may, at least in part, account for the difference in berenil binding affinities for the poly-[d(I-C)]$_2$ and poly[d(G-C)]$_2$ duplexes, which differ chemically only with respect to the presence or absence of an amino group at the C2 position of the purine base within the minor groove. Thus, the binding-induced hydrodynamic differences we observe between duplexes, as well as between the measured values and the theoretical limit for full intercalation, may reflect the presence of some partially intercalated drug molecules which manifest additional interactions within the groove(s). This interpretation represents another manifestation of mixed mode binding. A third potential contributor to the differential effects we observe could be berenil-induced conformational changes in the target duplexes which differentially alter the effective hydrodynamic length and stiffness of each target duplex. Such effects, in general, could cause a single binding mode to reflect properties characteristic of multiple binding modes. On the basis of the available data, we cannot differentiate between these alternative possibilities.

In stark contrast to the data we measure for the poly[d(A-T)]$_2$, poly[d(I-C)]$_2$, poly[d(G-C)]$_2$, and poly(rA)•poly(rU) duplexes, the length of the poly(dA)•poly(dT) duplex remains essentially unchanged up to an r_{bp} of 0.16 and then increases very slightly, reaching a plateau at an r_{bp} of 0.25. This contour length profile suggests that *berenil binds the poly(dA)•poly(dT) duplex nonintercalatively*. However, we cannot eliminate the alternative possibility of a fortuitous compensation in which berenil intercalates into the poly(dA)•poly(dT) duplex, while a binding-induced conformational change results in a decrease in contour length that just compensates the increase caused by drug intercalation. In fact, the slight increase in length observed between r_{bp} ratios of 0.16 and 0.25 may reflect a berenil-induced conformational change in the poly(dA)•poly(dT) duplex, perhaps from a noncanonical B′-conformation (Arnott & Selsing, 1974; Arnott et al., 1983; Alexeev et al., 1987; Park et al., 1987) to a more canonical B-conformation (Wilson et al., 1985; Breslauer et al., 1987; Herrera & Chaires, 1989; Scaria & Shafer, 1991).

The differential berenil binding modes suggested by our viscosity studies are similar to those observed by Wilson and co-workers (Wilson et al., 1990; Tanious et al., 1992) in studies on the nucleic acid-binding properties of DAPI, a chemically similar drug. In these studies, DAPI was shown to shown to exhibit both intercalative and minor groove binding properties in a nucleic acid sequence-dependent manner. Specifically, intercalation was observed at (dG-dC)$_n$•(dG-dC)$_n$ and (rA)$_n$•(rU)$_n$ sites, while minor groove binding was observed at (dA)$_n$•(dT)$_n$ sites. Our observation of similar duplex binding properties for berenil suggests that such mixed mode binding behavior may be general for ligands with structures similar to DAPI and berenil. This observation may be of practical significance since Liu and co-workers (Chen & Liu, 1994) have proposed that drugs which exhibit mixed modes of binding to duplex DNA also exhibit strong antitumor activities via topoisomerase I poisoning. If this correlation proves general, then biophysical studies such as described here and reported by Wilson and co-workers (Wilson et al., 1990; Tanious et al., 1992) may prove useful in screening for effective topoisomerase I poisoners.

Berenil Minor Groove Binding Appears To Require the Presence of at Least One 5′-ApA-3′ Dinucleotide Step. Crystallographic (Brown et al., 1990, 1992) and NMR (Yoshida et al., 1990; Shafer et al., 1990; Lane et al., 1991; Jenkins et al., 1993) studies on duplex DNA oligomers containing central regions of either four or six A•T base pairs, flanked on either side by two, three, or four G•C base pairs show that berenil binds within the minor grooves of the central A•T regions (these studies were conducted under ionic conditions which precluded berenil binding to the G•C regions of the oligomers). When the central A•T region is 5′-AATT-3′, the berenil molecule binds at the 5′-AAT-3′ site (Yoshida et al., 1990; Brown et al., 1990; Lane et al., 1991). When the central A•T region is 5′-AAATTT-3′, the berenil molecule binds at the 5′-AATT-3′ site (Lane et al., 1991; Brown et al., 1992). One interpretation of our viscometric results is that berenil intercalates at 5′-(AT)$_n$-3′ sequences, while binding in the minor groove of 5′-(A)$_n$-3′ sequences. Taken together, these data suggest that berenil binding in the minor groove of A•T sequences requires a minimum of one 5′-AA-3′ step. Such a requirement is not unreasonable since molecular modeling studies (Brown et al., 1992; Jenkins et al., 1993) suggest that differences in helical parameters, such as base pair roll and propeller twist, play a key role in determining the location of the berenil binding site when complexed in the minor groove at the 5′-AATT-3′ or 5′-AAATTT-3′ regions noted above. Such subtle structural differences in the duplex target also may influence the mode by which berenil binds to a target region containing other A•T sequences, such as 5′-(AT)$_n$-3′.

Berenil Binding Induces the Unwinding of Negative Supercoils in pBR322. Viscosity studies of berenil in which negatively supercoiled circular duplexes are used as targets provide another means of investigating the mode of berenil binding. Generally speaking, ligand intercalation into circular duplex DNA unwinds negative supercoils, ultimately creating a fully relaxed circular molecule, followed by formation of a positively supercoiled molecule (Crawford & Waring, 1967; Bauer & Vinograd, 1968; Waring, 1971). Such ligand-induced changes in tertiary structure are char-

acterized by an increase in viscosity upon unwinding of negative supercoils, followed by a decrease in viscosity with the formation of positive supercoils (Revet et al., 1971). The ratio of the total ligand to nucleotide concentration (r_{nuc}) at which the circular DNA molecule is fully relaxed is termed the critical saturation ratio, $\tilde{v}$.

Figure 5, panel B, shows the effect of either berenil, ethidium, or netropsin binding on the viscosity of a solution containing the negatively supercoiled plasmid pBR322. Note that, to ensure berenil interaction with *both* G·C and A·T sequences on the target plasmid, we conducted these viscosity experiments in 2 mM Na^+. Ethidium, a classic intercalating ligand known to strongly unwind negatively supercoiled DNA (Waring, 1965; Crawford & Waring, 1967; Wang, 1974; Liu & Wang, 1975; Keller, 1975), and netropsin, a classic minor groove-binding ligand known to only slightly wind negatively supercoiled DNA (Malcolm & Snounou, 1983; Snounou & Malcolm, 1983; Zimmer & Wähnert, 1986; Chen et al., 1993), were used as controls in the study. Addition of ethidium results in the expected viscosity profile for intercalation, with an observed critical saturation ratio ($\tilde{v}_E$) of 0.035, similar to the value of 0.037 reported by Crawford and Waring (1967) for the binding of ethidium to polyoma virus DNA. Addition of netropsin results in a decrease in solution viscosity, as expected from its tendency to wind negatively supercoiled DNA. At $r_{nuc} = 0.3-0.4$, netropsin induces a slight increase in viscosity which may be due to a secondary, nonspecific mode of binding (e.g., electrostatically driven binding at the helix exterior) that increases the stiffness of the DNA molecule. Such a secondary binding mode for netropsin previously has been proposed on the basis of acoustic measurements (Chalikian et al., 1994).

Inspection of panel B of Figure 5 reveals that the addition of berenil results in an initial increase in solution viscosity, reaching a maximum at a r_{nuc} ratio of 0.29, followed by a viscosity decrease. This viscosity profile is consistent with an intercalative mode of binding, with a critical saturation ratio ($\tilde{v}_B$) of 0.29. Note that the berenil-induced viscosity maximum is much broader and is shifted to a higher value of r_{nuc} than that induced by the classic intercalator ethidium. This observation is consistent with berenil intercalation at only select DNA sequences, in agreement with the viscosity profiles for the linear DNA targets shown in Figure 5, panel A. Wilson et al. (1990) have shown that the binding of DAPI to supercoiled DNA results in a viscosity profile in qualitative agreement with what we measure for berenil, with a similar critical saturation ratio of $\approx$0.32.

A lower estimate for the helix unwinding angle (ϕ_B) induced by berenil binding can be determined using the relationship (Cantor & Schimmel, 1980)

$$\phi_B \tilde{v}_B = \phi_E \tilde{v}_E \quad (4)$$

where ϕ_E is the helix unwinding angle of ethidium, known to be 26° (Wang, 1974; Liu & Wang, 1975; Keller 1975), and ϕ_B, $\tilde{v}_B$, and $\tilde{v}_E$ are as defined above. Using this approach, we calculate a ϕ_B value of $\geq$3.1°. This unwinding angle must be considered a lower estimate because not all of the bound berenil molecules necessarily employ the intercalative mode of binding.

The results of our viscosity studies on berenil binding to supercoiled DNA (pBR322) contrast with the observations of Waring (1970) based on sedimentation velocity (ultracentrifugation) studies of berenil binding to supercoiled ϕX174 RF DNA. In these studies, Waring observed a slight increase in Svedberg number (S_{20}) up to a r_{nuc} ratio of $\approx$0.1, followed by a small drop in S_{20} between r_{nuc} ratios of 0.1 and 0.13. This decrease in S_{20} at the last few points of the titration was attributed to the onset of aggregation (which precluded further addition of berenil beyond a r_{nuc} ratio of 0.13), and not to helix unwinding. Our observations suggest that this drop in S_{20} in fact reflects helix unwinding. If Waring had been able to carry the sedimentation velocity titration beyond an r_{nuc} ratio of 0.13, additional evidence for helix unwinding would have emerged.

Interestingly, we observe no evidence for precipitation or aggregation over the berenil concentration ranges used in our viscosity studies. Waring (1970) points out that the berenil preparation used in his sedimentation velocity studies was only 31% pure since it contained a stabilizer (antipyrene) that constituted 69% by weight of the drug preparation. This substantial impurity not only complicated his determination of accurate r_{nuc} ratios but also may have promoted the observed precipitation. Nevertheless, Waring estimates a helix unwinding angle for berenil of $\leq$2.3°, which he proposes sets a lower limit on the range of unwinding angles detectable by the sedimentation velocity experiment. In view of this sensitivity limit, our calculated helix unwinding angle of 3.1° for berenil suggests that the berenil-induced unwinding we have determined viscometrically approaches the detection limits of the ultracentrifugation technique and therefore might be undetected in a sedimentation velocity experiment.

CONCLUDING REMARKS

Based on previous studies, berenil has been classified as a minor groove binding ligand that is specific for AT-rich regions of B-form DNA (Portugal & Waring, 1986, 1987; Yoshida et al., 1990; Brown et al., 1990, 1992; Lane et al., 1991; Jenkins et al.,1993). We have used a combination of spectroscopic, calorimetric, and viscometric techniques to demonstrate here, that, under appropriate conditions, berenil can bind to both DNA and RNA duplexes and that this binding can exhibit properties characteristic of intercalative as well as minor groove-binding motifs.

Generally speaking, the results reported here have intrinsic value in that they contribute to the broad-based effort to define the molecular recognition patterns that control the affinities and specificities of nucleic acid binding ligands. Such knowledge is required for the ultimate development of a more rational approach to drug design. Our results also may have a more immediate and practical impact based on the suggestion by Liu and co-workers (Chen & Liu, 1994) that the ability of a drug to bind nucleic acids by multiple or "mixed" modes might be required for the drug to express chemotherapeutic activity through topoisomerase I poisoning. In fact, berenil already has been shown to be a potent inhibitor of viral, trypanosomal, and mammalian topoisomerases (Fairfield et al., 1979; Shaffer & Traktman, 1987; Sekiguchi & Kmiec, 1988). Thus, it may be possible to establish empirical correlations between the biophysical binding properties of a ligand and its biological activities, thereby providing a basis for drug screening.

ACKNOWLEDGMENT

We thank Dr. Slawomir Mielewczyk for assistance with the purification of berenil, Dr. George Strauss, in whose lab

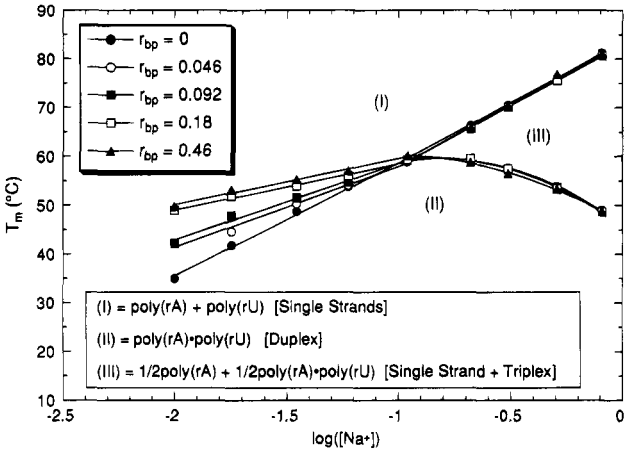

FIGURE A1: Phase diagram plotting T_m versus log [Na^+] for the poly(rA)•poly(rU) duplex and its complexes with berenil at the indicated values of r_{bp}. The structural states which correspond to each phase (I, II, or III) are indicated. Buffer conditions were 10 mM sodium cacodylate (pH 6.8) and 0.1 mM EDTA.

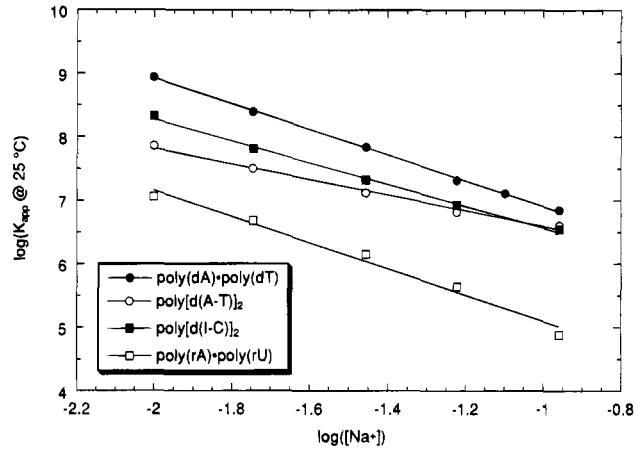

FIGURE A2: Salt dependence of berenil binding affinity. Log($K_{app}^{25°C}$) versus log [Na^+] plots for berenil binding to the poly(dA)•poly(dT) (filled circles), poly[d(A-T)]$_2$ (open circles), poly[d(I-C)]$_2$ (filled squares), and poly(rA)•poly(rU) (open squares) duplexes. These data were fit with eq A1 (solid line) to yield the results summarized in Table A1. In all cases, buffer conditions were 10 mM sodium cacodylate (pH 6.8) and 0.1 mM EDTA.

the viscometry experiments were conducted, Robert Porcja for assistance with setting up the viscometry apparatus, and Dr. Jean Baum for graciously allowing us use of the NMR facility. We also thank Jennifer Cohen, Stephanie Ritter, and Paula Adasczik for their participation in the preliminary studies which led to this investigation.

APPENDIX

Influence of Berenil Binding on the Poly(rA)•Poly(rU) Phase Diagram. Krakauer and Sturtevant (1968) previously have determined a phase diagram for the poly(rA)•poly(rU) duplex in the absence of drug binding. Their phase diagram mapped the salt dependence of the thermal stabilities (T_m) of the following three transitions:

$$\text{poly(rA)•poly(rU)} \rightleftharpoons \text{poly(rA)} + \text{poly(rU)} \quad \text{[WC]}$$

$$\text{poly(rA)•poly(rU)} \rightleftharpoons {}^1/_2\text{poly(rA)•poly(rU)} + {}^1/_2\text{poly(rA)} \quad \text{[DIS]}$$

$$\text{poly(rA)•2poly(rU)} \rightleftharpoons \text{poly(rA)} + 2\text{poly(rU)} \quad \text{[TSS]}$$

where DIS denotes the disproportionation transition and TSS denotes the triplex to single strand transition. In the first section of this Appendix, we expand their phase diagram by showing how these three equilibria are influenced by berenil binding. Such expanded phase diagrams are important for meaningfully defining and comparing nucleic acid binding properties over a range of solution conditions.

Figure A1 shows the effect of berenil binding on the phase diagram for the poly(rA)•poly(rU) duplex. Note that this expanded phase diagram exhibits a triple point at ≈110 mM Na^+. At Na^+ concentrations below the triple point, addition of berenil causes the T_m of the WC transitions to increase. The extent of this increase diminishes with increasing Na^+ concentration (ΔT_m = +12.8 °C in 10 mM Na^+, while ΔT_m = +2.3 °C in 60 mM Na^+ at an r_{bp} ratio of 0.46). Furthermore, the slopes, $\partial T_m/\partial \log([Na^+])$, of the lines that separate regions I and II (which correspond to the WC transition) are quite different for the drug-free and drug-bound duplexes (21.5 °C for the drug-free duplex and 8.6 °C for the drug-bound duplex at r_{bp} = 0.46). It is gratifying to note that the $\partial T_m/\partial \log([Na^+])$ values we have determined in the absence of drug for the WC transitions of poly(rA)•poly(rU) are consistent with previously reported values (Krakauer & Sturtevant, 1968; Record et al., 1976; Chou, 1990).

Further inspection of the phase diagram reveals that, at Na^+ concentrations above the triple point (110 mM Na^+), both families of lines overlap. Thus, berenil binding has virtually no effect on the T_m values of either the DIS transition (phase II → phase III) or the TSS (phase III → phase I) transition. These observations may be due to a salt-induced reduction in the extent of berenil binding to both the poly(rA)•poly(rU) duplex and the poly(rA)•2poly(rU) triplex. The average slope of the lines corresponding to the TSS transitions in the presence and absence of drug is 25.2 °C. This value is in agreement with those observed by others for the drug-free triplex to single-strand transition of this molecule (Krakauer & Sturtevant, 1968; Record et al., 1976). To normalize such slope comparisons for differences in transition enthalpies, differential scanning calorimetric studies on the berenil/poly(rA)•poly(rU) complex must be conducted so that one can calculate the thermodynamic degree of ion dissociation (Δi) for each transition (Record et al., 1976).

The results presented above describe the influence of berenil binding on the salt- and temperature-dependent transitions of an RNA duplex, namely, poly(rA)•poly(rU). As noted above, such phase diagrams are important when defining and comparing the nucleic acid binding properties of ligands over a range of solution conditions. In fact, as described below, one can use the data associated with such phase diagrams to evaluate the extent to which charge interactions contribute to the nucleic acid binding affinity of a ligand by examining the salt dependence of the binding constants.

Electrostatic Contributions of Berenil Binding to Duplex Structures. Figure A2 shows the Na^+ dependence of berenil binding to the poly(dA)•poly(dT), poly[d(A-T)]$_2$, poly[d(I-C)]$_2$, and poly(rA)•poly(rU) host duplexes. The observed linear dependencies can be described by the relationship (Record et al., 1978; Anderson & Record, 1983).

$$\log K_{app} = -Z_{app}\psi\{\log([Na^+])\} + \log K^\circ \quad \text{(A1)}$$

where Z_{app} is the apparent valence of berenil, ψ is the

Table A1: Electrostatic Contributions to the Complexation of Berenil with Various Double-Helical Nucleic Acids

host duplex	axial rise per residue[a] (Å)	b^c (Å)	ψ^c	$-Z_{app}\psi^{b,c}$	$Z_{app}{}^c$	log $K°$ [b]
poly(dA)·poly(dT)	3.29	1.65	0.88	−2.02	2.30	4.90
poly[d(A-T)]$_2$	3.03	1.52	0.89	−1.23	1.38	5.37
poly[d(I-C)]$_2$	3.04	1.52	0.89	−1.71	1.92	4.86
poly(rA)·poly(rU)	2.81	1.41	0.90	−2.07	2.30	3.03

[a] Values for the axial rise per residue were derived from the following published X-ray fiber diffraction studies: Arnott and Selsing (1974) for poly(dA)·poly(dT), Arnott et al. (1974) for both poly[d(A-T)]$_2$ and poly[d(I-C)]$_2$, and Arnott et al. (1973) for poly(rA)·poly(rU). [b] Values for $-Z_{app}\psi$ and log $K°$ were derived, respectively, from the slopes and the y intercepts of the log K_{app} versus log [Na+] plots shown in Figure A2. [c] b is the average spacing of negative charges on the nucleic acid molecule; ψ is the thermodynamic counterion binding parameter and is equal to $1 - (2\xi)^{-1}$, where ξ is the axial charge density of the nucleic acid molecule and is equal to 7.14 Å/b; and Z_{app} is the apparent valence of berenil.

thermodynamic counterion binding parameter [which equals $1 - (2\xi)^{-1}$, where ξ is the the axial charge density of the nucleic acid structure], and K° is the equilibrium constant for the reaction

$$\text{berenil} + \text{duplex} \overset{K°}{\rightleftharpoons} \text{berenil/duplex} + Z_{app}\psi[Na^+]$$

Use of eq A1 to analyze the log($K_{app}^{25°C}$) versus log [Na^+] plots shown in Figure A2 yields the $-Z_{app}\psi$ (slope) and log $K°$ (y intercept) values summarized in Table A1. Note that, depending on the host duplex, the $-Z_{app}\psi$ values range from −1.23 to −2.07. In conjunction with the appropriate ψ values listed in Table A1, we calculate that when bound to the host duplexes the apparent valence of berenil (Z_{app}) ranges from 1.4 to 2.3. These results suggest that, qualitatively speaking, both charged ends of berenil participate electrostatically in its binding to each duplex, with the quantitative extent of the electrostatic contribution being dependent on the specific host structure. The Z_{app} value of 1.4 for berenil binding to the poly[d(A-T)]$_2$ duplex compared with 2.3 for the corresponding binding to the poly(dA)·poly(dT) or poly(rA)·poly(rU) duplexes suggests less electrostatic contributions from one or both of the charged amidino groups within the berenil/poly[d(A-T)]$_2$ complex. This result is consistent with that of Schmitz and Hübner (1993), who report weaker electrostatic contributions to berenil complexation to the poly[d(A-T)]$_2$ than to the poly(dA)·poly(dT) duplex.

Manning (1978, 1979) has shown that the *nonspecific* binding of a divalent cation to a B-DNA duplex is accompanied by a log $K°$ value (y intercept) of 0.40. Inspection of the data in Table A1 reveals that the log $K°$ values we determine for berenil binding to the poly[d(A-T)]$_2$ (5.36), the poly[d(I-C)]$_2$ (4.86), and the poly(dA)·poly(dT) (4.90) duplexes differ markedly from this prediction, suggesting that berenil binding to each duplex is associated with large electrostatic contributions from *site-specific* interactions. We previously observed a similar result for the binding of two steroid diamines to duplex DNA (Marky et al., 1983a). With regard to the one RNA host duplex, Record and co-workers (1978) have shown that *nonspecific* binding of a divalent cation to poly(rA)·poly(rU) yields a log $K°$ value of 1.17, in marked contrast to the corresponding log $K°$ value of 3.03 that we measure. Thus, as we observed when DNA served as the host duplex, berenil binding to duplex RNA also appears to be accompanied by large electrostatic contributions from *site-specific* interactions.

SUPPORTING INFORMATION AVAILABLE

^{1}H NMR spectra of berenil in D_2O as a function of total drug concentration and temperature, analyzed to assess the concentration-dependent aggregation state of berenil and to calculate the associated thermodynamics of the self association process (7 pages). Ordering information is given on any current masthead page.

REFERENCES

Alexeev, D. G., Lipanov, A. A., & Skuratovskii, I. Ya. (1987) *Nature 325*, 821−823.

Anderson, C. F., & Record, M. T., Jr. (1983) in *Structure and Dynamics: Nucleic Acids and Proteins* (Clementi, E., & Sarma, R. H., Eds.) pp 301−319, Adenine Press, New York.

Arnott, S., & Selsing, E. (1974) *J. Mol. Biol. 88*, 509−521.

Arnott, S., Hukins, D. W. L., Dover, S. D., Fuller, W., & Hodgson, A. R. (1973) *J. Mol. Biol. 81*, 107−122.

Arnott, S., Chandrasekaran, R., Hukins, D. W. L., Smith, P. J. C., & Watts, L. (1974) *J. Mol. Biol. 88*, 523−533.

Arnott, S., Chandrasekaran, R., Hall, I. H., & Puigjaner, L. C. (1983) *Nucleic Acids Res. 11*, 4141−4155.

Baker, B. T., & Erickson, E. H. (1967) *J. Am. Chem. Soc. 10*, 1123−1128.

Barceló, F., & Portugal, J. (1993) *Biophys. Chem. 47*, 251−260.

Barton, J. K., Goldberg, J. M., Kumar, C. V., & Turro, N. J. (1986) *J. Am. Chem. Soc. 108*, 2081−2088.

Bauer, W., & Vinograd, J. (1968) *J. Mol. Biol. 33*, 141−171.

Bloomfield, V. A., Crothers, D. M., & Tinoco, I., Jr. (1974) *Physical Chemistry of Nucleic Acids*, pp 442−445, Harper & Row, New York.

Braithwaite, A., & Baguley, B. C. (1980) *Biochemistry 19*, 1101−1106.

Braswell, E., & Lary, J. (1981) *J. Phys. Chem. 85*, 1573−1578.

Breslauer, K. J., Remeta, D. P., Chou, W.-Y., Ferrante, R., Curry, J., Zaunczkowski, D., Snyder, J. G., & Marky, L. A. (1987) *Proc. Natl. Acad. Sci. U.S.A. 84*, 8922−8926.

Broder, S. (1989) in *Concepts in Viral Pathogenesis III* (Notkins, A. L., & Oldstone, M. B. A., Eds.) pp 337−351, Springer-Verlag, New York.

Brown, D. G., Sanderson, M. R., Skelly, J. V., Jenkins, T. C., Brown, T., Garman, E., Stuart, D. I., & Neidle, S. (1990) *EMBO J. 9*, 1329−1334.

Brown, D. G., Sanderson, M. R., Garman, E., & Neidle, S. (1992) *J. Mol. Biol. 226*, 481−490.

Cantor, C. R., & Schimmel, P. R. (1980) *Biophysical Chemistry, Part III: The Behavior of Biological Macromolecules*, pp 1265−1290, W. H. Freeman, New York.

Chaires, J. B., Dattagupta, N., & Crothers, D. M. (1982) *Biochemistry 21*, 3927−3932.

Chalikian, T. V., Sarvazyan, A. P., Plum, G. E., & Breslauer, K. J. (1994) *Biochemistry 33*, 8629−8640.

Chen, A. Y., & Liu, L. F. (1994) *Annu. Rev. Pharmacol. Toxicol. 34*, 191−218.

Chen, A. Y., Yu, C., Bodley, A., Peng, L. F., & Liu, L. F. (1993) *Cancer Res. 53*, 1332−1337.

Chou, W.-Y. (1990) Ph.D. Thesis, Rutgers University, New Brunswick, NJ.

Chou, W.-Y., Marky, L. A., Zaunczkowski, D., & Breslauer, K. J. (1987) *J. Biomol. Struct. Dyn. 5*, 345−359.

Cohen, G., & Eisenberg, H. (1969) *Biopolymers 8*, 45−55.

Crawford, L. V., & Waring, M. J. (1967) *J. Mol. Biol. 25*, 23−30.

Crothers, D. M. (1971) *Biopolymers 10*, 2147−2160.

Crothers, D. M., Sabol, S. L., Ratner, D. I., & Müller, W. (1968) *Biochemistry 7*, 1817−1822.

Dervan, P. B. (1986) *Science 232*, 464−471.

Dimicoli, J.-L., & Hélène, C. (1973) *J. Am. Chem. Soc. 95*, 1036−1044.

Eriksson, S., Kim, S. K., Kubista, M., & Nordén, B. (1993) *Biochemistry 32*, 2987−2998.

Fairfield, F. R., Bauer, W. R., & Simpson, M. V. (1979) *J. Biol. Chem. 254*, 9352−9354.

Gale, E. F., Cundiffe, E., Reynolds, P. E., Richmond, M. H., & Waring, M. J. (1981) *The Molecular Basis of Antibiotic Action*, 2nd ed., pp 258−401, Wiley, New York.
Glasoe, P. K., & Long, F. A. (1960) *J. Phys. Chem. 64*, 188−190.
Gulbransen, E. A., & Robinson, A. L. (1934) *J. Am. Chem. Soc. 56*, 2637−2641.
Guschlbauer, W., & Saenger W., Eds. (1987) *DNA−Ligand Interactions: From Drugs to Proteins*, Plenum Press, New York.
Herrera, J. E., & Chaires, J. B. (1989) *Biochemistry 28*, 1993−2000.
Hélène, C., & Toulmé, J.-J. (1990) *Biochim. Biophys. Acta 1049*, 99−125.
Hélène, C., Montenay-Garestier, T., Saison, T., Takasugi, M., Toulmé, J.-J., Asseline, U., Lancelot, G., Maurizot, J.-C., Toulmé, F., & Thuong, N. T. (1985) *Biochimie 67*, 777−783.
Jenkins, T. C., Lane, A. N., Neidle, S., & Brown, D. G. (1993) *Eur. J. Biochem. 213*, 1175−1184.
Jin, R. (1989) Ph.D. Thesis, Rutgers University, New Brunswick, NJ.
Job, P. (1928) *Ann. Chim. (Paris) 9*, 113−134.
Jones, R. L., Lanier, A. C., Keel, R. A., & Wilson, W. D. (1980) *Nucleic Acids Res. 8*, 1613−1624.
Kallenbach, N. R., Ed. (1988) *Chemistry & Physics of DNA−Ligand Interactions*, Adenine Press, New York.
Keller, W. (1975) *Proc. Natl. Acad. Sci. U.S.A. 72*, 4876−4880.
Krakauer, H., & Sturtevant, J. M. (1968) *Biopolymers 6*, 491−512.
Lane, A. N., Jenkins, T. C., Brown, T., & Neidle, S. (1991) *Biochemistry 30*, 1372−1385.
Lerman, L. S. (1961) *J. Mol. Biol. 3*, 18−30.
Liu, L. F., & Wang, J. C. (1975) *Biochim. Biophys. Acta 395*, 405−412.
Malcolm, A. D. B., & Snounou, G. (1983) *Cold Spring Harbor Symp. Quant. Biol. 47*, 323−326.
Manning, G. S. (1978) *Q. Rev. Biophys. 11*, 179−246.
Manning, G. S. (1979) *Biopolymers 18*, 2357−2358.
Marky, L. A., & Breslauer, K. J. (1987a) *Biopolymers 26*, 1601−1620.
Marky, L. A., & Breslauer, K. J. (1987b) *Proc. Natl. Acad. Sci. U.S.A. 84*, 4359−4363.
Marky, L. A., Snyder, J. G., & Breslauer, K. J. (1983a) *Nucleic Acids Res. 11*, 5701−5715.
Marky, L. A., Snyder, J. G., Remeta, D. P., & Breslauer, K. J. (1983b) *J. Biomol. Struct. Dyn. 1*, 487−507.
McGhee, J. D., & von Hippel, P. H. (1974) *J. Mol. Biol. 86*, 469−489.
Mitsuya, H., Yarchoan, R., & Broder, S. (1990) *Science 249*, 1533−1544.
Müller, W., & Crothers, D. M. (1968) *J. Mol. Biol. 35*, 251−290.
Neidle, S., & Abraham, Z. (1984) *CRC Crit. Rev. Biochem. 17*, 73−121.
Newton, B. A. (1967) *Biochem. J. 105*, 50P-51P.
Park, H.-S., Arnott, S., Chandrasekaran, R., Millane, R. P., & Campagnari, F. (1987) *J. Mol. Biol. 197*, 513−523.
Park, Y.-W. (1992) Ph.D. Thesis, Rutgers University, New Brunswick, NJ.
Pearl, L. H., Skelly, J. V., Hudson, B. D., & Neidle, S. (1987) *Nucleic Acids Res. 15*, 3469−3478.
Pilch, D. S., Levenson, C., & Shafer, R. H. (1990) *Proc. Natl. Acad. Sci. U.S.A. 87*, 1942−1946.
Pilch, D. S., Martin, M.-T., Nguyen, C.-H., Sun, J.-S., Bisagni, E., Garestier, T., & Hélène, C. (1994) *J. Am. Chem. Soc. 115*, 9942−9951.
Portugal, J., & Waring, M. J. (1986) *Nucleic Acids Res. 14*, 8735−8754.
Portugal, J., & Waring, M. J. (1987) *Eur. J. Biochem. 167*, 281−289.
Record, M. T., Jr., Woodbury, C. P., & Lohman, T. M. (1976) *Biopolymers 15*, 893−915.
Record, M. T., Jr., Anderson, C. F., & Lohman, T. M. (1978) *Q. Rev. Biophys. 11*, 103−178.
Remeta, D. P., Mudd, C. P., Berger, R. L., & Breslauer, K. J. (1991) *Biochemistry 30*, 9799−9809
Remeta, D. P., Mudd, C. P., Berger, R. L., & Breslauer, K. J. (1993) *Biochemistry 32*, 5064−5073.
Revet, B. M., Schmir, M., & Vinograd, J. (1971) *Nature 229*, 10−13.
Riley, M., Maling, B., & Chamberlin, M. J. (1966) *J. Mol. Biol. 20*, 359−389.
Robinson, A. L. (1932) *J. Am. Chem. Soc. 54*, 1311−1318.
Scaria, P. V., & Shafer, R. H. (1991) *J. Biol. Chem. 266*, 5417−5423.
Schmitz, H. U., & Hübner, W. (1993) *Biophys. Chem. 48*, 61−74.
Schwarz, G., & Stankowski, S. (1979) *Biophys. Chem. 10*, 173−181.
Sekiguchi, J. A. M., & Kmiec, E. B. (1988) *Mol. Cell. Biochem. 83*, 195−205.
Shaffer, R., & Traktman, P. (1987) *J. Biol. Chem. 262*, 9309−9315.
Shafer, R. H., Yoshida, M., Banville, D. L., & Hu, S. (1990) in *Molecular Basis of Specificity in Nucleic Acid-Drug Interactions* (Pullman, B., & Jortner, J. Eds.) pp 59−65, Kluwer Academic Publishers, Dordrecht, The Netherlands.
Shigehiro, S., & Takusagawa, F. (1994) *J. Am. Chem. Soc. 116*, 4154−4165.
Snounou, G., & Malcolm, A. D. B. (1983) *J. Mol. Biol. 167*, 211−216.
Snyder, J. G. (1989) Ph.D. Thesis, Rutgers University, New Brunswick, NJ.
Snyder, J. G., Hartman, N. G., D'Estantoit, B. L., Kennard, O., Remeta, D. P., & Breslauer, K. J. (1989) *Proc. Natl. Acad. Sci. U.S.A. 86*, 3968−3972.
Stein, C. A., & Cohen, J. S. (1988) *Cancer Res. 48*, 2659−2668.
Tanious, F. A., Veal, J. M., Buczak, H., Ratmeyer, L. S., & Wilson, W. D. (1992) *Biochemistry 31*, 3103−3112.
Toulmé, J.-J., & Hélène, C. (1988) *Gene 72*, 51−58.
Wang, J. C. (1974) *J. Mol. Biol. 89*, 783−801.
Waring, M. J. (1965) *J. Mol. Biol. 13*, 269−282.
Waring, M. J. (1970) *J. Mol. Biol. 54*, 247−279.
Waring, M. J. (1971) *Prog. Mol. Subcell. Biol. 2*, 216−231.
Wells, R. D., & Larson, J. E. (1970) *J. Mol. Biol. 49*, 319−342.
Wilson, W. D., Wang, Y.-H., Krishnamoorthy, C. R., & Smith, J. C. (1985) *Biochemistry 24*, 3991−3999.
Wilson, W. D., Tanious, F. A., Barton, H. J., Jones, R. L., Fox, K., Wydra, R. L., & Strekowski, L. (1990) *Biochemistry 29*, 8452−8461.
Wiseman, T., Williston, S., Brandts, J. F., & Lin, L.-N. (1989) *Anal. Biochem. 179*, 131−137.
Yoshida, M., Banville, D. L., & Shafer, R. H. (1990) *Biochemistry 29*, 6585−6592.
Zhou, N., James, T. L., & Shafer, R. H. (1989) *Biochemistry 28*, 5231−5239.
Zimmer, C. (1975) *Prog. Nucleic Acids Res. Mol. Biol. 15*, 285−318.
Zimmer, C., & Wähnert, U. (1986) *Prog. Biophys. Mol. Biol. 47*, 31−112.

BI950715S